2005

Effect of multiuser interference on subscriber location in CDMA networks

Rohit Sharma
Louisiana State University and Agricultural and Mechanical College

EFFECT OF MULTIUSER INTERFERENCE ON SUBSCRIBER LOCATION IN CDMA NETWORKS

A Thesis

Submitted to the Graduate Faculty of
the Louisiana State University and
Agricultural and Mechanical College
in partial fulfillment of the
requirements for the degree of
Master of Science in Electrical Engineering

in

The Department of Electrical Engineering

by
Rohit Sharma
B.E., Mumbai University, India, 2001
May 2005

Acknowledgements

First and foremost, I would like to extend my deepest thanks and gratitude to my advisor Dr.Morteza Naraghi-Pour for his academic guidance and support. Right from the time I started working on my thesis, he has been very helpful in organizing my ideas and putting together a very fine piece of work. Also, I am grateful for his patience in reading, and correcting my errors in thesis writing.

I also like to thank to Dr. Xue-Bin Liang and Dr. Guoxiang GU for being a very supportive committee.

I thank my parents Mr.Chandrakant Sharma and Mrs.Pratima Sharma, my sister Shruti, for making me believe in myself and encourage me to pursue my Masters degree. Their blessings, guidance and love have brought me a long way in my life.

I would like to thank Mahesh, Seema and Srinath for patiently proof reading my thesis. I would like to thank Rhett, my computer manager, for helping me with network storage, remote connections and other computer related issues.

Finally I must express my deepest appreciation to everyone, for their support and encouragement.

Table of Contents

List of Tables

List of Figures

Abstract

The last few years have witnessed an ever growing interest in the field of mobile location systems for cellular systems. The motivation is the series of regulations passed by Federal Communications Commission, requiring that wireless service providers support a mobile telephone callback feature and cell site location mechanism. A further application of the location technology is in the rapidly emerging field of intelligent transportation systems, which are intended to enhance highway safety, location based billing etc.
Many of the existing location technologies use GPS and its derivatives which require a specialized subscriber equipment. This is not feasible for popular use, as the cost of such equipments is very high. Hence, for a CDMA network, various methods have been studied that use the cellular network as the sole means to locate the mobile station (MS), where the estimates are derived from the signal transmitted by the MS to a set of base station's (BS) This approach has the advantage of requiring no modifications to the subscriber equipment. While subscriber location has been previously studied for CDMA networks, the effect of multiple access interference has been ignored. In this thesis we investigate the problem of subscriber location in the presence of multiple access interference. Using MATLAB as a simulation tool, we have developed an extensive simulation technique which measures the error in location estimation for different network and user configurations. In our studies we include the effects of log-normal shadow and Rayleigh fading. We present results that illustrate the effects of varying shadowing losses, number of BS's involved in position location, early-late discriminator offset and cell sizes in conjunction with the varying number of users per cell on the accuracy of radiolocation estimation.

Chapter 1

Overview of Subscriber Location

The spatial properties of wireless channels are very important in determining the performance of a subscriber location system. In this chapter we would be looking at the most commonly used channel models like macro-cellular and micro-cellular channel models, followed by an overview of radio propagation environment. Later we would look at the most commonly used subscriber location techniques and conclude with the most useful technique as far as CDMA cellular networks are concerned.

1.1 Wireless Channel Models

In this section, a few realistic spatial channels are introduced, and the defining equations and the key results are described. There are various models developed, each catering to a realm of applications. More information about the various channel models can be obtained at [8].

1.1.1 Macrocell Model

In a macro-cellular environment it is usually assumed that the scatterers around the MS are usually of the same height as or higher than the MS. This implies that the received signal at the MS arrives from all directions and hence is assumed to have an uniform distribution over $[-\pi, \pi]$ [5] [6]. But the situation is different at the BS. In a macro-cellular environment it is assumed that the BS is deployed above the surrounding scatterers and hence the multi path components at the BS are restricted to a smaller angular region, and the direction of arrival is no longer uniform over $[-\pi, \pi]$. Jakes [5] and Gans [7] have modeled the macro-cellular environment as a ring of scatterers around the MS but with BS outside this ring. Fig.1.1 [1] illustrates this geometry. Scatterers are assumed to be present on a ring of radius a around the MS, and the BS is assumed to be at a distance d from MS, such that $d >> a$. Assuming that MS uses an omni directional antenna, distribution for signals arriving at BS $p(\theta)$ is given by [1]

$$p(\theta) = \begin{cases} K\sqrt{[(\frac{a}{d})^2 - (\beta - \theta)^2]} & \beta - \theta_M \leq \theta \leq \beta + \theta_m \\ 0 & otherwise \end{cases}$$

where,

$$\theta_M = \arctan(\frac{a}{d})$$

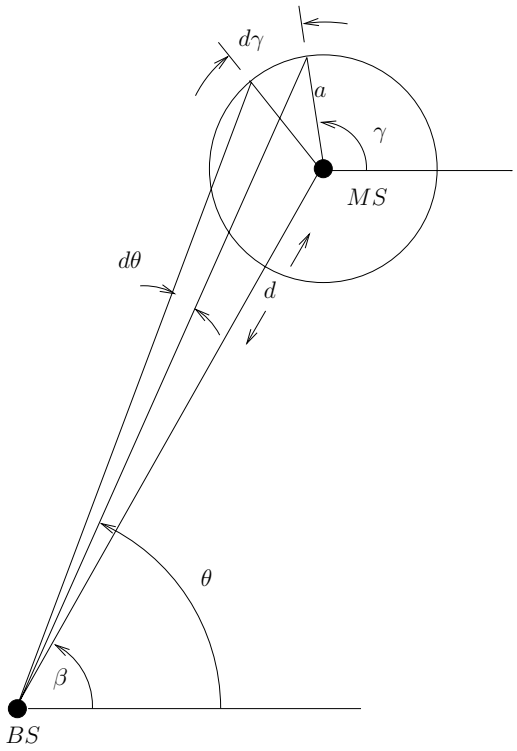

Figure 1.1: MS-BS Geometry Assuming a Ring of Scatterers for Macrocells

$$K = \frac{1}{2\arcsin(\frac{d\theta_M}{a})}$$

For $d >> a$, we can approximate θ_M as

$$\theta_M \approx \frac{a}{d}$$

giving

$$K \approx \frac{1}{\pi}$$

For MS this model predicts a relatively high probability of multipath components with small excess delays along the line of sight. From the BS perspective, all of the multi path components are restricted to lie within a small range of angles. Measurements reported in [8] suggest that typical angular spreads at BS for macro-cellular environment with T-R separation of 1Km, approximate to 2 to 6 degrees.

This model can be used to generate sample channels for simulation processes. Generation can be done by uniformly placing scatterers in a circular scatter region around the MS and then calculating the corresponding direction of arrival, time of arrival and power levels.

1.1.2 Microcell Model

A micro-cell model assumes BS as well as MS to be surrounded by scatterers. Thus, the angular spread of the received signals at the BS is much higher in micro cells than in macro cells. The situation in a micro cellular environment can be modeled as an ellipse with BS and MS located at the foci of ellipse [8]. Fig. 1.2 represents geometrical interpretation of a Maricela model. In

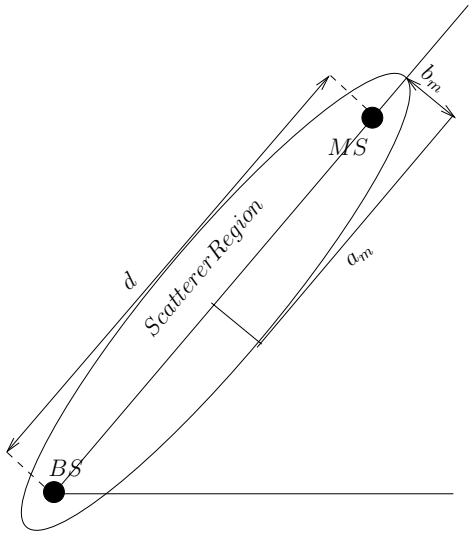

Figure 1.2: MS-BS Geometry for Microcells

a micro cellular environment antenna heights are very low, hence multi path scattering is just as likely near the BS as it is near the MS. An essential feature of micro cellular model is that it considers multi path signals that arrive with a delay ≤ a chosen value of maximum delay τ_m [8]. This assumption is logical, as components with longer delays correspond to longer path lengths, which experience higher path losses. If τ_m is chosen sufficiently large, model would take into consideration nearly all the power and DOA of multi path components. If a_m and b_m represent major and minor axis of the ellipse containing the scatterers,

$$a_m = \frac{c\tau_m}{2} b_m = \sqrt{c^2\tau_m^2 - d^2} \tag{1.1}$$

where c is the speed of light. The power-delay-angle profile obtained from this model is given by [8]:

$$f_{\tau,\phi}(\tau,\phi) = \begin{cases} \frac{(d^2-\tau^2c^2)(d^2c-2dc\tau^2\cos(\phi)+\tau^2c^3)}{4\pi a_m b_m (d\cos\phi - c\tau)^3} & \frac{d}{c} < \tau < \tau_m \\ 0 & otherwise \end{cases}$$

This model is used to simulate power-delay-angle profiles, power-delay profiles, joint marginal characteristics of direction of arrival and narrow band fading envelopes.

1.2 Radio Propagation Environment

Radio signals generally propagate according to three mechanisms: reflections, diffraction and scattering. As a result, radio propagation can be characterized by 3 nearly independent phenomenons

1. Path Loss
2. Slow Log Normal Shadowing
3. Small scale fading

1.2.1 Path Loss

Both theoretical and measurement based propagation models indicate that the intensity of an electromagnetic wave in free space decays with the square of radio path length d. The received power at a distance d is given by

$$\Omega_p(d) = \Omega_t k(\frac{\lambda_c}{4\pi d})^2 \tag{1.2}$$

where Ω_t is the transmitted power, λ_c is the wavelength and k is a constant of proportionality. These losses are categorized under 'Large Scale Losses'. Simplest path loss model assumes that the received power is

$$\Omega_p(d) = \Omega_p(d_0) - 10m\log(\frac{d}{d_0}) \tag{1.3}$$

where $\Omega_p(d_0)$ is the average received power at a known reference distance d_0. The parameter m is called the path loss exponent. For any transmitter and a receiver these losses are expressed as a function of of the distance 'd', by using a path loss exponent 'm'. Value of m dictates the rate at which the signal strength decays with distance. Typically for free space communications value of m is assumed to be 2. In real world scenario value of path loss exponent depends on the cell size and local terrain. Its value varies between 3 to 4 for a macro cellular environment and between 2 to 8 for a micro cellular environment. Table 1.1 [16] lists Path Loss Exponents for different environments.

In our model we are considering $m = 4$.

1.2.2 Slow Log-normal Shadowing

Equation (1.3) can not be directly used in estimation of Path Losses. This is a result of varying environment clutter. Measurements have shown that at any value of d, the path loss at a particular location is random and distributed log-normally about the mean distance dependent value. The simplest path loss model assumes that [21]

$$\Omega_p(d) = \mu_{\Omega_p(dBm)}(d_0) - 10m\log(\frac{d}{d_0})(dBm) + \epsilon_{(dB)}(dBm) \tag{1.4}$$

where

Table 1.1: Path Loss Exponents for different Environments

Environment	Path Loss Exponent, m
Free Space	2
Urban area cellular radio	2.7 to 3.5
Shadowed urban cellular radio	3 to 5
In building line of sight	1.6 to 1.8
Obstructed in building	4 to 6
Obstructed in factories	2 to 3

- $\mu_{\Omega_{p(dBm)}}(d_0)$ is the average received signal power at a known reference distance d_0. This average power would depend on the frequency, antenna heights, their gains and other factors.
- m is the path loss exponent factor.
- $\epsilon_{(dB)}$ is a zero mean Gaussian random variable in dB that represents the error between actual and estimated path loss. Variation in its value is caused due to shadowing.

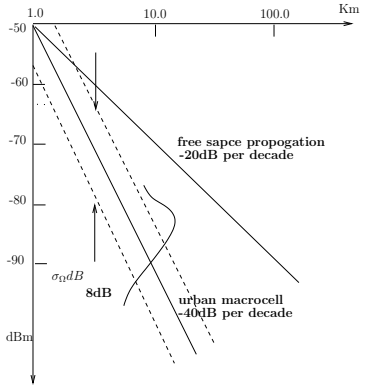

Figure 1.3: Path Loss in Free Space and Macrocellular Environments, β=4, σ_Ω=8dB

Shadows are generally log-normally distributed, and their probability density function is given by [21]

$$p_{\Omega_{p(dBm)}}(d)(x) = \frac{1}{\sqrt{2\pi}\sigma_\Omega} exp\{-\frac{(x - \mu_{\Omega_{p(dBm)}}(d))^2}{2\sigma_\Omega^2}\} \tag{1.5}$$

where,

$$\mu_{\Omega_{p(dBm)}}(d) = \mu_{\Omega_{p(dBm)}}(d_0) - 10m\log(\frac{d}{d_0})(dBm) \tag{1.6}$$

and, σ_Ω is the shadow standard deviation. Fig. 1.3 [21] illustrates the variation in signal strength with distance in presence and absence of shadowing. Usually σ_Ω ranges from 4 to 12 dB with 8dB being its typical value.

1.2.3 Small Scale Fading

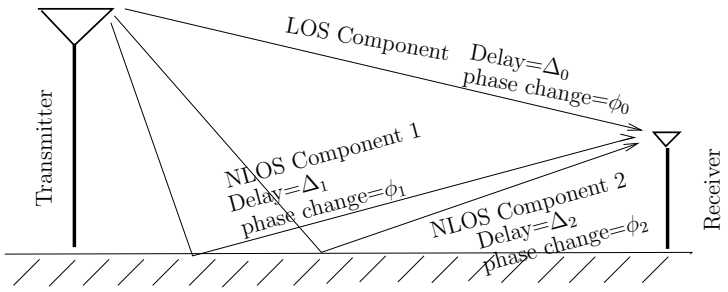

Figure 1.4: Multipath Propagation

As can be seen from Fig. 1.4 plane waves at receiver arrive from many directions with different delays and phase angles. This phenomenon is described as multi path propagation. Thus at the receiver, all these multiple copies vectorially combine to produce a composite received signal as shown in Fig. 1.5. Mobile communication uses radio frequencies with wavelengths in orders of ten's of centimeters. Hence, small changes in differential propagation delays lead to changes in the phase of arriving plane waves. Hence the waves undergo a constructive and destructive interference at the receiver. As a result the signal experiences rapid fluctuations in

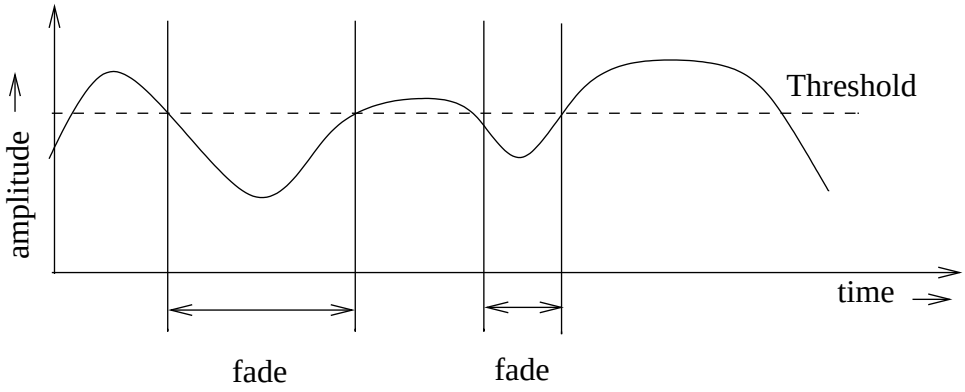

Figure 1.5: Received Signal at Receiver due to Multipath Propagation

amplitude over a short period of time, as can be seen in Fig. 1.5. Such an effect leads to fading often referred to as multi path fading or small scale fading.

Multipaths in radio channel result in the following:

1. Rapid changes in signal strength over a small period or distance.

2. Random frequency shifts on different multi path signals, thereby leading to a form of frequency modulation. These random frequency shifts in the multi path versions of the signal are refereed to as Doppler shifts. These Doppler shifts are a result of relative motion between the transmitter and receiver. Fig. 1.6 illustrates one such situation, where a MS

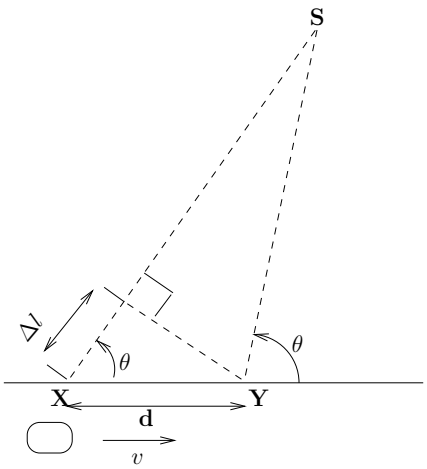

Figure 1.6: Doppler Spread in Cellular Networks

moves with a constant velocity v from X to Y along a path of length d. It is receiving signals from a remote source S. The difference in path lengths traveled by the wave from source S to points X and Y is

$$\begin{aligned} \Delta l &= d\cos\theta \\ &= v\Delta t\cos\theta \end{aligned} \tag{1.7}$$

where Δt is the time required for the MS to travel from X to Y and θ is assumed to be constant over distance Δl. The phase change in the received signal due to difference in path lengths is

$$\begin{aligned} \Delta\phi &= \frac{2\pi\Delta l}{\lambda} \\ &= \frac{2\pi v\Delta t}{\lambda}\cos\theta \end{aligned} \tag{1.8}$$

and hence the apparent change in frequency or Doppler shift is given by

$$\begin{aligned} f_d &= \frac{1}{2\pi}\frac{\Delta\phi}{\Delta t} \\ &= \frac{v}{\lambda}\cos\theta \end{aligned} \tag{1.9}$$

3. Time dispersion caused by the multi path propagation delays. This can be explained as broadening of a pulse due to time delay as shown in Fig. 1.7.

Small scale fading can be further classified into frequency non-selective or flat and frequency selective fading.

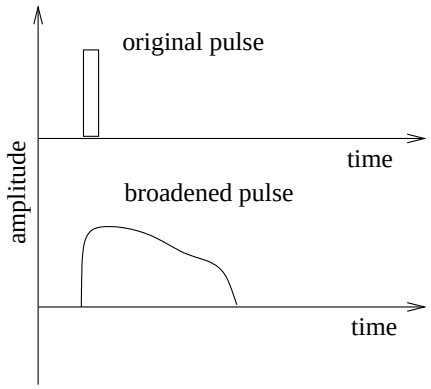

Figure 1.7: Time Dispersion in Transmitted Pulse due to Multipath Propagation

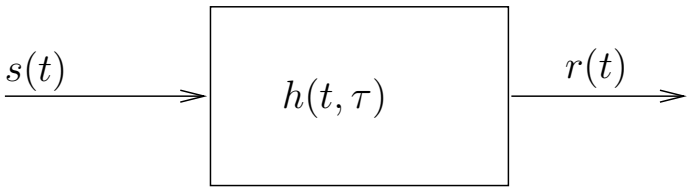

Figure 1.8: Flat Fading Channel Characteristics

- Flat fading: If the mobile radio channel has a constant gain and linear phase response over a bandwidth which is greater than the bandwidth of the transmitted signal, then the received signal would undergo flat fading [16]. The characteristics of a flat fading channel can be illustrated as shown in Fig. 1.8. Thus, in a flat faded channel, amplitude of the received signal may change with time but the frequency spectra is preserved. Flat fading channels are also referred to as amplitude varying or narrow band channels, since the bandwidth of signal is narrow as compared to channel bandwidth. The most commonly encountered amplitude distributions belong to the category of flat fading are Rayleigh, Rician and Nakagami fading.

- Frequency selective fading: If the channel possesses a constant gain and linear phase response over a bandwidth that is smaller than the bandwidth of the transmitted signal, then the channel creates frequency selective fading over the signal [16]. When this occurs, received signal consists of multiple versions of original waveform that are attenuated and delayed in time, thereby distorting the received signal. Thus, the channel introduces intersymbol interference (ISI). When viewed in frequency domain, certain frequency components in the received signal spectrum have greater gains than others. Frequency selective fading channels are also refered to as wide-band channels as the bandwidth of the transmitted signal is more than the bandwidth of the channel impulse response.

1.3 Overview of Subscriber Location

The art of subscriber location in a wireless network is also termed as ”Radiolocation”. It involves the following:

1. Identifying the BS’s that would participate in the process of subscriber location. This involves selection of a set of BS’s within the coverage area that receive intelligible levels of signal from the MS under consideration. Normally three or more BS’s from coverage area are selected for subscriber location.

2. Estimating 1-D position: Each BS, participating in the process, independently produces an estimate of the subscriber location based on its measurements.

3. Location estimation: Estimates from all the participating BS’s are then used by position location algorithms to produce an accurate estimate of the subscriber location within the coverage area.

But, the estimates produced are not always very accurate. The major sources of error in subscriber location systems are

- Multi path Propagation: Multi path propagation is a primary source of error in position location techniques. Accuracy is greatly affected when the reflected rays arrive within a very small period of the first arriving ray. Case is even more worsened when the power of reflected rays is more than the first arriving ray. Several methods have been developed to mitigate the effects of multi path on radiolocation. The most recent being super resolution techniques such as Root-MUSIC [13] and TLS-ESPIRIT algorithms [9]. Other developed techniques are based on Extended Kalman Filtering [10], High-resolution frequency estimation [12], and Least Mean Square [11] approach.

- Non-line-of-sight propagation: Typically Non-line-of-sight (NLOS) propagation in wireless communications accrue up to an average of 400-700m [14] and bias the estimations. Hence it is necessary to distinguish between a NLOS and a line of sight (LOS) component. By using the a priori information about range error statistics, range estimations made over a period of time and corrupted by NLOS errors can be adjusted to near their correct values. An alternative approach is to reduce the weights of the BS’s prone to NLOS reception while estimating location using position location algorithms [1].

- Multiple Access Interference: Co-channel interference is a problem faced by all the cellular systems. In CDMA users share the same frequency band, but use unique PN codes. Near far effects in CDMA networks are the biggest source of errors in position estimation. Multiple access interference (MAI) greatly effects the performance of ToA estimation systems. We have tried to study the effects of MAI on accuracy of subscriber location systems. More about effect of MAI on subscriber location will be discussed in subsequent chapters.

The following parameters of a radio signal can be used to perform Radiolocation,

- Signal Strength
- Angle of Arrival (AOA)
- Time of arrival (ToA)

Let us briefly look into each of the above methods.

1.3.1 Signal Strength

This method makes use of known mathematical models describing signal attenuation with distance [2][3]. Thus by exploiting the one-to-one relationship between the signal strength and distance, an estimate of the distance is obtained. The MS lies on a circle centered at the BS and radius equal to the estimated distance. By using multiple BS's, MS location can be estimated.

This method of estimation assumes the following:

- Signal attenuation is only due to path loss.
- The path loss model is known and is deterministic.

But, in real world situations the aforementioned assumptions fail. In a radio environment the path loss depends not only on distance but also on the antenna heights of the BS and MS, and terrain characteristics such as buildings, hills etc. The site specific dependence of radio propagation makes the theoretical prediction of path loss difficult. As a combined effect of all these losses signal strength may vary as much as 30-40dB over distances of about half wavelength. Effect of these variable losses can be minimized by making use of premeasured contours centered at the BS [4]. Method of contours assumes the following

- Topography around the BS remains constant
- All the BS's within the coverage area have such contours

Plotting these contours for every base station within the coverage area is a time consuming and tedious job. Moreover, these contours are subject to change every time the topography around the BS changes. Thus, it is a less attractive approach especially for a micro cellular environment, where the number of BS's within a coverage area are much more.

1.3.2 Angle of Arrival

Angle of Arrival (AoA) or Direction of Arrival (DoA) techniques constitute a class of position location systems called direction finding systems. These techniques restrict the location of a MS along a line in the estimated DoA. As shown in Fig. 1.9 when multiple AoA measurements are made at multiple locations, location of the MS can be estimated by intersection of their line of bearings. In theory, we need only two BS to estimate the MS location, but in practice due to the channel impairments, discussed earlier, more than 2 sensors are required.

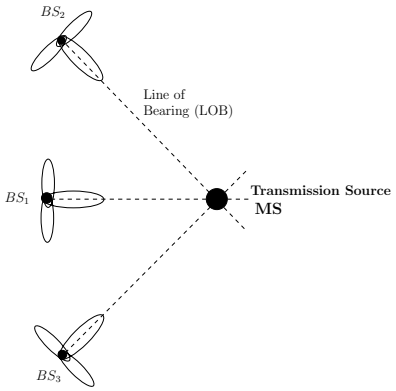

Figure 1.9: 2-D AoA Position Locator

AoA measurements can be made by using antenna arrays or super resolution techniques. The antenna arrays to be used for AoA measurements should have large apertures and must bear large number of elements. Also, for increased accuracy they must be able to provide a high angular resolution. AoA measurements can suffer from radio channel impairments such as multi path propagation, NLoS reception and MAI. In AoA measurement systems the direction of source is usually chosen to be the one of the strongest arriving signal component. In systems that also estimate multi path delays, the direction of source is estimated using the first resolvable multi path component.

The problem is elevated when estimation is carried out in a micro cellular environment where the BS's are usually surrounded by a number of local scatterers. In such shadowed areas the LOS signal may be completely obstructed by the surrounding environment and only multi path components of the signal may be detectable, resulting in the arrival of signal at the BS with greater angular spreads. In such cases, the estimate will be along the strongest or the first resolvable multi path component, which leads to error in estimated MS location. The situation is slightly better for macro cells. In a macro cell the scattering objects are primarily within a small distance of the MS, as the BS's are usually elevated well above the local terrain [5], [6]. Jakes [5] and Gans [7] have modeled this situation.

Though we may use AoA technique in a macro cellular environment, it is impractical to use it in micro cellular environment. Also, accuracy of estimation in using AoA technique reduces as distance between MS and BS increases [1]. Moreover, the methods used for AoA estimation necessitate the use of complex signal processing methods for estimation.

1.3.3 Time of Arrival

Time of Arrival (ToA) constitutes a class of position location methods called 'True Ranging Position Location' systems. It measures the exact distance between a MS and a set of BS's through the use of Time of Arrival (ToA) of the signal. Distance between a BS and a MS is equal to the product of the velocity of the radio signal and the time it takes to reach the BS from the

MS, i.e.,

$$R_i = c\tau_i \tag{1.10}$$

where, R_i is the range measurement, c is the speed of light, τ_i is the ToA estimate at the i^{th} receiver. Thus, if a measurement was made, MS must lie on the periphery of a circle centered at the measuring BS and radius equal to the estimated distance. An exact estimation of location can be made using triangulation, as shown in figure 1.10

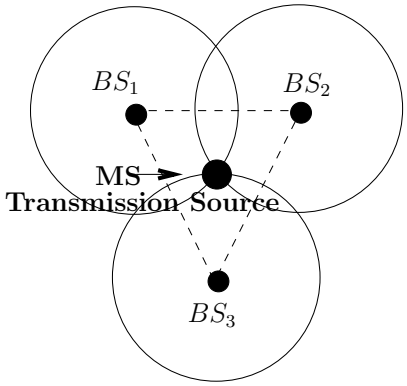

Figure 1.10: 2-D ToA Position Locator

The accuracy of subscriber location is directly related to the accuracy of the ToA estimation. Both GSM and CDMA systems use PN sequences. In GSM every burst consists of a pre determined 26 bit PN sequence. Thus at a BS, the receiver synchronizes the locally generated PN sequence with the received PN sequence and estimates the delay in received signal. Similar to this, in a CDMA network the receiver synchronizes itself with the received PN sequence and thus estimates the delay.

For systems employing PN codes, we could

1. estimate a coarse timing using a sliding correlator or matched filter

2. estimate fine time using a delay locked loop or tau dither loop

[1]. Since finer estimates can be obtained from delay locked loop's (DLL), they are better suited for ToA estimations in radiolocation systems.

Fig. 1.11 outlines the structure of a typical DLL employed in ToA estimations. It allows synchronization of locally generated PN sequence with the incoming code. It generates a local code and correlates the incoming PN code with the early and late versions of the locally generated code. Shown in Fig. 1.12 are the autocorrelations of the early and late codes, where N represents the length of the PN code.

The accuracy with which the DLL can track the incoming PN code depends on a parameter Δ called the 'Early-Late' discriminator offset. The early and late PN sequences are separated by a period equal to $2\Delta T_c$. The code phase error signal $e(t)$ is obtained by squaring and differencing the correlator outputs. The squaring operations remove the effect of modulation and carrier phase

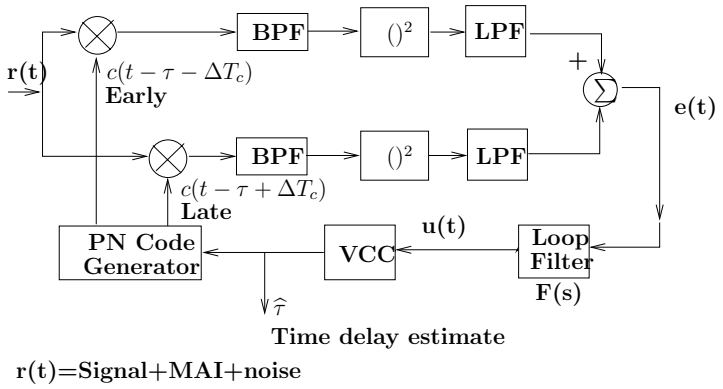

Figure 1.11: Non Coherent DLL used for Time Based Subscriber Location

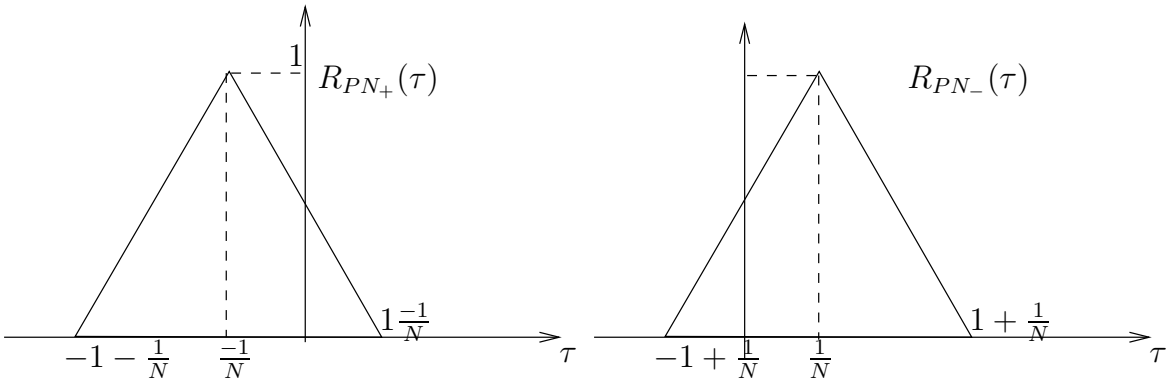

Figure 1.12: Autocorrelation Functions of the Early and Late PN code

shift [1]. This error signal is then passed through a low pass filter, to eliminate the high frequency components and obtain the signal $u(t)$. $u(t)$ drives the voltage controlled clock (VCC) to correct the code phase error of locally generated code. Also the level and polarity of this signal provides an estimate of $\hat{\tau}$. Fig. 1.13 is the discriminator characteristic curve for the DLL, shown in Fig. 1.11. Let $\hat{\tau}$ represent the value of τ for which the DLL is synchronized with the incoming PN sequence. At $\tau = \hat{\tau}$, $u(t) = 0$.

Once an estimate of ToA is obtained, the next step is position location. The simplest approach in position estimation using ToA estimate is the geometric approach which computes the point of intersection of circles of ToA, as shown in Fig. 1.14. The location of MS is the point of intersection of the circles. But, this would happen only when the ToA estimates are exact which in practice is rarely possible due to

- Effects of MAI, NLOS propagation and multi path fading.
- Accuracy of the employed delay estimation techniques.

In practice the situation is as shown in Fig. 1.14. The circles do not intersect at one common point. As can be seen there are three points of intersections. In such cases location estimate is

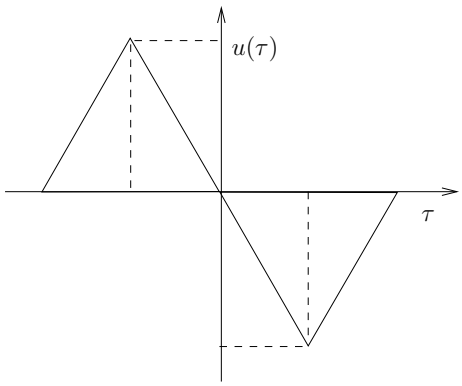

Figure 1.13: Discriminator Characteristic

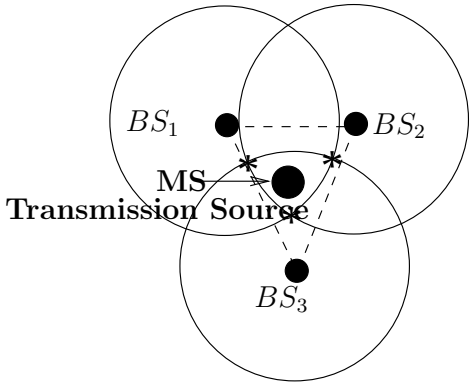

Figure 1.14: Ambiguity in Radiolocation, as all the Circles do not Intersect at one point

derived by finding out the centroid of the triangle so formed.

To improve the accuracy of estimation, we use more than three BS's. In such a case, estimation of position using geometric approach is very difficult. In practice a popular method for estimating MS location is using the method of non-linear least squares (NLLS) [1]. This approach assumes that the MS located at (x_0, y_0) transmits the signal at time τ_0. There are N BS's located at (x_1, y_1), (x_2, y_2),.....(x_N, y_N), involved in the process of subscriber location. They receive the transmitted signal at times τ_1, τ_2,.....τ_N, respectively. As a performance measure we consider the function [1]

$$f_i(\mathbf{z}) = c(\tau_i - \hat{\tau}) - \sqrt{(x_i - \hat{x})^2 + (y_i - \hat{y})^2} \tag{1.11}$$

where c is the speed of light, and

$$\mathbf{z} = [\hat{x}, \hat{y}, \hat{\tau}].$$

Basically, $f_i(\mathbf{z})$ is an estimation of the error between the actual distance $c(\tau_i - \tau_0)$ of MS from BS i at (x_i, y_i) (based on ToA estimate, τ_i), and the estimated distance $\sqrt{(x_i - \hat{x})^2 + (y_i - \hat{y})^2}$, where $(\hat{x},\hat{y})$ represent the estimated location of the MS. Note that if the estimated values of $(\hat{x},\hat{y})$ and $\hat{\tau}$ coincide with the actual position of MS and actual time τ_0 at which the signal was transmitted,

then $f_i(\mathbf{z})$ is zero. However, the estimated values of ToA's $\hat{\tau}_i$ are in error. Hence to obtain a location estimate based on raw ToA estimate the following cost function is used [1],

$$F(\mathbf{z}) = \sum_{i=1}^{N} \alpha_i^2 f_i^2(x) \tag{1.12}$$

where α_i are the weights that can be chosen to reflect the reliability of a BS in estimating τ_i. If a BS used in position location is prone to heavy multi path and NLOS losses due to its terrain and topography, we could choose a lower value of α for it. A location estimate is obtained by minimizing the cost function $F(\mathbf{z})$ given in (1.12).

1.3.4 TDoA Estimation

Similar to the ToA approach, there is a TDoA (Time Difference of Arrival) approach, which makes use of difference of ToA's at the participating BS's. In TDoA approach, the BS's are located at the foci of the hyperbola on which the MS must lie. Making use of triangulation, an exact MS location can be found. Relationship between the range difference and the TDoA measurement between the receivers is given by

$$\begin{aligned} R_{i,j} &= c\tau_{i,j} \\ &= c(\tau_i - \tau_j) \\ &= R_i - R_j \end{aligned} \tag{1.13}$$

where $\tau_{i,j}$ is TDoA between receiver i and j, $R_{i,j}$ is the range difference, τ_i and τ_j are ToA arrival estimates at BS i and j, while R_i and R_j are range estimates at BS i and j. Figure 1.15 illustrates a TDoA estimation in 2-D.

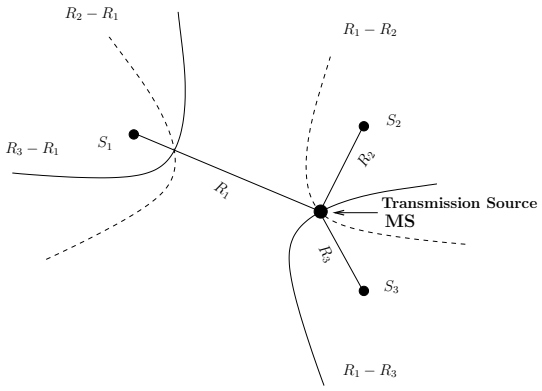

Figure 1.15: 2-D TDoA Position Locator

There are 2 ways of obtaining TDoA estimates [8]. The first way is subtracting the ToA estimates from two BS to produce a relative TDoA estimate. But this requires a knowledge of

timing at the 2 BS's and thus requires a strict clock synchronization between the two BS's. Fortunately, this is available in CDMA networks. Also, this method has an advantage of eliminating the errors in ToA estimates common to all the BS's. While, determining the TDoA estimates from ToA estimates is feasible for some air interfaces, the second method that makes use of the cross correlation estimation technique is the predominantly used technique for deriving TDoA estimate. Consider a signal $s(t)$ being radiated by a MS and being received by two BS [8].

Let

$$\begin{aligned} r_1(t) &= C_1 s(t - d_1) + n_1(t) \\ r_2(t) &= C_2 s(t - d_2) + n_2(t) \end{aligned} \tag{1.14}$$

represent the received signals at the two BS's. C_1 and C_2 are the scaled amplitudes of the received signals with delays d_1 and d_2, corrupted with noise $n_1(t)$ and $n_2(t)$. It is assumed that $s(t)$, $n_1(t)$ and $n_2(t)$ are real and jointly stationary, zero mean random processes and that $s(t)$, $n_1(t)$ and $n_2(t)$ are uncorrelated. Assuming $d_1 < d_2$, (1.14) can be rewritten as

$$\begin{aligned} r_1(t) &= s(t) + n_1(t) \\ r_2(t) &= As(t - d) + n_2(t) \end{aligned} \tag{1.15}$$

where A is the amplitude ratio between the two received signals and $d = d_2 - d_1$. TDoA estimation requires estimation of values of d.

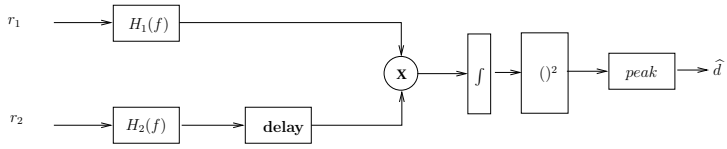

Figure 1.16: Generalized Cross Correlation Method for TDoA estimation

A generalized cross correlation approach is shown in Fig. 1.16. In the most simplest form, excluding the two filters shown in Fig. 1.16, the cross correlation function of these two received signals is

$$C(\tau) = \frac{1}{T} \int_0^T r_1(t) r_2(t + \tau) dt \tag{1.16}$$

TDoA estimate $\hat{d}$ is the value of τ that maximizes the cross correlation. This approach requires analog signals $r_1(t)$ and $r_2(t)$ to be sent to a common processing site. Also, since estimation due to TDoA does not require the BS's to be synchronized in time, it can be applied in narrow band cellular systems like GSM for subscriber location.

Once the TDoA estimate is found, a hyperbolic position location algorithm is used to produce an accurate and unambiguous solution to the position location algorithm. In our work we have evaluated the performance of position location techniques using ToA estimates and hence we would not be discussing the hyperbolic position location techniques in detail. For further reading on hyperbolic position location estimation techniques, reader is directed to [8].

1.4 Subscriber Location in CDMA systems

Section 1.3 outlines various methods can be used for subscriber location in a cellular environment. In CDMA cellular systems the MS's are power controlled to combat the near-far effect. Hence we can not use the estimation method based on signal strengths in a home cell, as the signals from all the MS within the home cell would be received with the same strength at the home BS. AOA method could find application in systems requiring lower accuracies. With increased multi path interference and poor LOS reception in a micro cellular environment, AOA proves to be a very ineffective method for radiolocation in micro cells. Also estimation of angle of arrival by means of an antenna array is a complicated process. It requires a complicated antenna design and extensive signal processing. For TDoA systems, the signals received at the BS's must be transmitted to a common processing site. This increases the overheads on the BS's. Alternatively ToA methods could be used. The only drawback they face is the requirement of high timing resolution equipment. But for a CDMA cellular network more accurate time estimates can be derived because they employ PN sequences.

Thus, for a CDMA network, time based approach is the most promising technique. Our discussion in the subsequent chapters would be based on subscriber location using ToA approach.

Chapter 2

Approximating MAI in CDMA Networks

2.1 Multiple Access Interferences in CDMA Networks

In a CDMA system all the users share the same frequency band. As a result, at a CDMA receiver signals from users, other than the intended user, act as interfering signals, thereby giving rise to multiple access interference. Fig. 2.1 represents such a situation.

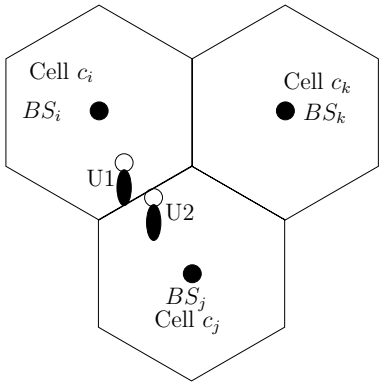

Figure 2.1: Coverage Area

With reference to Fig. 2.1, the coverage area comprises of three cells, C_i, C_j and C_k. These cells have n_i, n_j and n_k users respectively. The BS's i, j and k exercise power control over the users they serve. Let A_i, A_j and A_k denote their areas. Only three cells have been considered for simplicity of explaination.

Multiple access interference within a coverage area can be broadly classified as:

- Intracellular interference: Intracell interference experienced at a BS is caused by the users in the same cell. This is mainly caused due to the non orthogonality in the PN codes assigned to the users. For instance, consider cell C_i. At BS i while processing the signal from user $U1$, signals from the other $n_i - 1$ users, power controlled by BS i, would act as interferes. A mathematical expression for the intracellular multiple access interference would be derived in subsequent sections.

- Intercellular interference: Intercell interference experienced at a BS, is caused by the users in other cells. These users are power controlled by another BS. It is assumed that the power control overcomes shadowing losses and large scale losses. Users within a cell are all power controlled by the same BS and hence the received power at the controlling BS, from the users it power controls, is same and is equal to the nominal power. For instance, consider cell C_i. The received power due to all the n_i users of cell C_i at BS i would be the same and be equal to nominal power P. Same is the case with the n_j users of cell C_j at BS j. But, the received powers of n_i users, power controlled by BS i , at BS j would not be the same. The power received at BS j from user $U1$, power controlled by BS i, at the edge of cell i, would be comparable to the power received from user $U2$, even though it is not power controlled by BS j. Thus, it will act as an interferer at BS j. Similar will be the case with all the users of cell i. Such an interference is called intercellular interference. We would derive a mathematical expression for the same in subsequent sections.

2.2 Modeling Intracellular Multiple Access Interference at the Receiver Output

Let us derive a mathematical model for the intracellular multiple access interference caused due to the $n_p - 1$ users of some cell C_p, at its BS p. In a CDMA system using binary signaling, the radio signal from the k^{th} user, arriving at the BS is given by:

$$s_k(t - \tau_k) = \sqrt{2P_k}c_k(t - \tau_k)b_k(t - \tau_k)\cos(\omega_c t + \phi_k) \tag{2.1}$$

where,

- P_k is the power received from the k^{th} user at the BS. Assuming, perfect power control is exercised, we can replace P_k by P, where P represents the nominal power received at the BS from a user under its power control.
- $c_k(t)$ is the spreading (or chip) sequence for a user k.
- $b_k(t)$ is the data sequence for a user k.
- τ_k is the delay for user k relative to a user 0.
- ϕ_k is the phase change for user k relative to a user 0.
- ω_c is the carrier frequency.

In the above equation we assume that there is no multi path interference in the channel.

A PN sequence $c_k(t)$ is of the form: [16]

$$c_k(t) = \sum_{j=-\infty}^{\infty}\sum_{i=0}^{M-1} a_{k,i}\Pi\left(\frac{t - (i + jM)T_c}{T_c}\right) \tag{2.2}$$

$$a_{k,i} \in \{-1, 1\}$$

where,

- T_c represents the chip duration.
- MT_c represents the chip repetition period.
- Π represents the unit pulse function given by

$$\Pi(t) = \begin{cases} 0 \leq t \leq 1 \\ 0 \qquad otherwise \end{cases} \tag{2.3}$$

- i is an index to denote a particular chip within a PN cycle.

For data sequence $b_k(t)$, T_b is the bit period such that

$$T_b = GT_c$$

where G represents the spreading factor or gain of the CDMA system. It is not necessary that the gain G of a CDMA system be equal to M. In case they are same, a PN sequence would be repeated for every bit period T_b.

The user data sequence $b_k(t)$ is given by

$$b_k(t) = \sum_{j=-\infty}^{\infty} b_{k,j}\Pi(\frac{t - jT_b}{T_b}) \tag{2.4}$$
$$b_{k,j} \in \{-1, 1\}$$

Figure 2.2 is a model for CDMA multiple access interference. As can be seen from Fig.2.2, the signal received at the BS is given by

$$r(t) = \sum_{k=0}^{n_p-1} s_k(t - \tau_k) + n(t) \tag{2.5}$$

where

- n(t) represents a zero-mean white Gaussian noise with two sided power spectral density $N_0/2$.
- n_p represents the number of users power controlled by BS p.

To derive a decision statistic, the received signal $r(t)$ is mixed with the baseband, multiplied with the PN sequence of the desired user, and integrated over the bit period T_b. Assuming that the receiver is phase and delay synchronized with the k^{th} user, the output of the correlator can be written as, [16]

$$Z_k = \int_{jT_b}^{(j+1)T_b} r(t)c_k(t)\cos(\omega_c t)dt \tag{2.6}$$

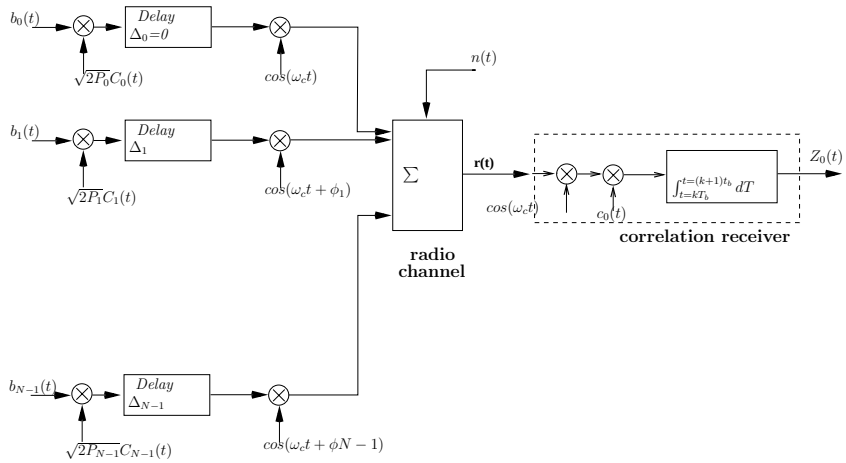

Figure 2.2: Model for CDMA Intracellular Multiple Access Interference

Assume that the receiver is phase and delay synchronized with the k^{th} user, for simplicity we would assume τ_k=0, and ϕ_k=0. For simplicity of notation, we assume that the desired user is user 0. Hence k=0.

Substituting equation's (2.1) and (2.5) in equation (2.6) we obtain

$$\begin{aligned} Z_0 &= \int_{t=0}^{T_b} [r(t)c_0(t)\cos(\omega_c t)]dt \\ &= \int_{t=0}^{T_b} [(\sum_{k=0}^{n_p-1} s_k(t-\tau_k)+n(t))c_0(t)\cos(\omega_c t)]dt \\ &= \int_{t=0}^{T_b} [(\sum_{k=0}^{n_p-1} \sqrt{2P_k}c_k(t-\tau_k)b_k(t-\tau_k)\cos(\omega_c t+\phi_k))+n(t)]c_0(t)\cos(\omega_c t)dt \end{aligned} \quad (2.7)$$

Z_0 is a decision statistic for the desired user.

We may express equation (2.7) as

$$Z_0 = I_0 + \zeta + \eta \quad (2.8)$$

where,

1. I_0 is the contribution from the desired user, i.e.,

$$I_0 = \int_{t=0}^{T_b} \sqrt{2P_0}b_0(t)c_0^2(t)\cos^2(\omega_c t)dt$$

As $c_k \in$ {-1,1}, c_k^2=1.

Hence expression for I_0 reduces to

$$I_0 = \sqrt{\frac{P_0}{2}} b_0(t) T_b \tag{2.9}$$

2. ζ represents the contribution of multiple access interference and is the summation of $n_p - 1$ terms, I_k, where

$$I_k = \int_{t=0}^{T_b} \sqrt{2P_k} c_k(t - \tau_k) b_k(t - \tau_k) \cos(\omega_c t + \phi_k) c_0(t) \cos(\omega_c t) dt \tag{2.10}$$

$$\zeta = \sum_{k=1}^{n_p - 1} I_k \tag{2.11}$$

3. η represents the contribution of noise and is given by

$$\eta = \int_{t=0}^{T_b} n(t) c_0(t) \cos(\omega_c t) dt \tag{2.12}$$

Let us determine the variance and mean of η.

$$\mu_\eta = E[\eta] = \int_{t=0}^{T_b} E[n(t)] c_0(t) \cos(\omega_c t) dt = 0 \tag{2.13}$$

Variance of η can be computed as

$$\sigma_\eta^2 = E[(\eta - \mu_\eta)^2] = E[\eta^2]$$

$$= E[\int_{\lambda=0}^{T_b} \int_{t=0}^{Tb} n(t) n(\lambda) c_0(\lambda) \cos(\omega_c \lambda) c_0(t) \cos(\omega_c t) dt d\lambda]$$

$$= \int_{\lambda=0}^{T_b} \int_{t=0}^{Tb} E[n(t) n(\lambda)] c_0(\lambda) \cos(\omega_c \lambda) c_0(t) \cos(\omega_c t) dt d\lambda]$$

Now,

$$E[n(t) n(\lambda)] = \frac{N_0}{2} \delta(t - \lambda)$$

Hence

$$\sigma_\eta^2 = \int_{\lambda=0}^{T_b} \int_{t=0}^{Tb} \frac{N_0}{2} c_0(\lambda) \cos(\omega_c \lambda) c_0(t) \cos(\omega_c t) \delta(t - \lambda) dt d\lambda$$

$$\sigma_\eta^2 = \int_{t=0}^{T_b} \frac{N_0}{2} c_0^2(t) \cos^2(\omega_c t) dt$$

$c_0^2(t) = 1$. Hence

$$\sigma_\eta^2 = \int_{t=0}^{T_b} \frac{N_0}{4} (1 + \cos(2\omega_c t))$$

$$\sigma_\eta^2 = \frac{N_0 T_b}{4} \tag{2.14}$$

2.2.1 Gaussian Approximation of Intracellular MAI Present at the Correlator Output

Assuming a large number of interferes, by virtue of the central limit theorem (CLT), the distribution of ζ can be approximated by a zero-mean Gaussian distribution [16] with variance σ_ζ^2 given by [16]

$$\sigma_{\zeta^2} = \frac{GT_c^2 \sum_{k=1}^{n_p-1} P}{6} \tag{2.15}$$

Let,

$$\xi = \zeta + \eta \tag{2.16}$$

define the combined noise and intracellular interference at the receiver output. Assuming that the

ξ represnts total noise present at the correlator output (excluding intercellular noise)
ζ represents the intracellular interference component of total noise
η represents thermal noise

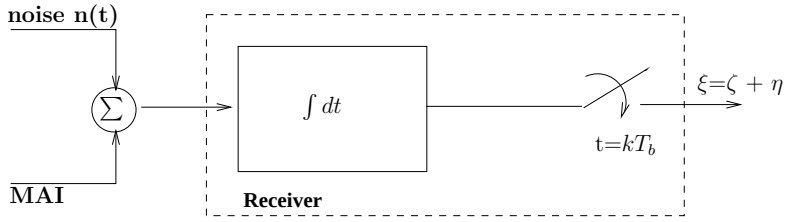

Figure 2.3: Representation of Noise Present at the Correlator Output

multiple access interference and noise are independent processes, the variance of ξ can be written as

$$\sigma_\xi^2 = \sigma_\zeta^2 + \sigma_\eta^2 \tag{2.17}$$

$$= \frac{GT_c^2 \sum_{k=1}^{n_p-1} P}{6} + \frac{N_0 T_b}{4} \tag{2.18}$$

2.3 Modeling Intercellular Multiple Access Interference

Let us derive an expression for the intercellular interference caused by the users of cell C_i at BS j. Let us represent this by I_{ij}. Let the user $U1$, shown in fig. 3.2 be located at M(x,y). Let the path loss exponent be m. Let the fading on path from this user to cell C_i be Rayleigh distributed, and represented by χ_i . Similarly, let the fading on the path from this user to cell C_j be Rayleigh distributed, and represented by χ_j. The average of $\chi_\mathbf{i}^\mathbf{2}$ is the log-normal fading on the path from this user to cell i, i.e, $E[\chi_i^2|\zeta_i] = 10^{-\zeta_i/10}$, where ζ_i is the decibel attenuation due to shadowing, and is a Gaussian random variable with zero-mean and standard deviation σ_s [18]. Similarly the

average of χ_j^2 is the log-normal fading on the path from this user to cell j. Let P be the nominal power received at BS i from user $U1$.

It is assumed that the power control mechanism overcomes both the large scale path loss and shadow fading. However, it does not overcome fast fluctuations of signal power due to Rayleigh fading [17]. As BS i exercises a power control over the MS, the actual transmission power of the MS would be

$$P \times r_i(x,y)^m 10^{\zeta_i/10} \tag{2.19}$$

where $r_i(x,y)$ is the distance of the MS from BS i. Consequently, assuming an uniform user density in the cell, the relative average interference at cell C_j caused by all the users in cell C_i is given by [19]

$$I_{ij} = E[\frac{n_i}{A_i} \int\int_{C_i} \frac{r_i^m(x,y) \times 10^{\zeta_i/10}}{\frac{r_j^m(x,y)}{\chi_j^2}} dA(x,y)] \tag{2.20}$$

The expectation is calculated as follows:
Using iterated expectations,

$$E[10^{\frac{\zeta_i}{10}}.\chi_j^2] = E[E[10^{\frac{\zeta_i}{10}}.\chi_j^2|\zeta_i,\zeta_j]]$$

$$= E_{\zeta_i\zeta_j}[E[10^{\frac{\zeta_i}{10}}\chi_j^2|\zeta_i\zeta_j]]$$

$$= E_{\zeta_i\zeta_j}[10^{\frac{\zeta_i}{10}}E[\chi_j^2|\zeta_i,\zeta_j]]$$

Given ζ_i and ζ_j,

$$E[\chi_j^2|\zeta_i,\zeta_j]$$

is log normal and is equal to

$$10^{-\frac{\zeta_j}{10}}$$

Thus,

$$E[10^{\frac{\zeta_i}{10}}.\chi_j^2] = E[10^{\frac{(\zeta_i-\zeta_j)}{10}}]$$

Let X= ζ_i - ζ_j.
Thus, X is a Gaussian variable of zero-mean and variance equal to $2\sigma_s^2$.

$$E[10^{\frac{\zeta_i}{10}}.\chi_j^2] = E[e^{\gamma x}]$$

$$E[10^{\frac{\zeta_i}{10}}.\chi_j^2] = \int_{-\infty}^{\infty} \frac{e^{\gamma x} e^{\frac{\gamma x^2}{4\sigma_s^2}}}{\sqrt{4\pi\sigma_s^2}} dx$$

$$E[10^{\frac{\zeta_i}{10}}.\chi_j^2] = e^{(\gamma\sigma_s)^2} \tag{2.21}$$

where $\gamma = \ln(10)/10$. Substituting the result back in (2.20) we obtain

$$I_{ij} = e^{(\gamma\sigma_s)^2} \frac{n_i}{A_i} \int\int_{C_i} \frac{r_i^m(x,y)}{r_j^m(x,y)} dA(x,y) \tag{2.22}$$

If α denotes the voice activity factor, then the above equation becomes

$$I_{ij} = e^{(\gamma\sigma_s)^2} \frac{n_i \alpha}{A_i} \int\int_{C_i} \frac{r_i^m(x,y)}{r_j^m(x,y)} dA(x,y) \tag{2.23}$$

Let κ_{ij} denote inter-cell interference factor due to a user in cell i at BS j.
Hence,

$$\kappa_{ij} = \frac{I_{ij}}{n_i} \tag{2.24}$$

$$= e^{(\gamma\sigma_s)^2} \frac{\alpha}{A_i} \int\int_{C_i} \frac{r_i^m(x,y)}{r_j^m(x,y)} dA(x,y) \tag{2.25}$$

Note, that in our model κ_{ii} is zero. It is important to point out the importance of κ_{ij}. κ_{ij} gives the interference at BS j caused by a single user in cell i. Thus, if the total number of users in cell i were to change, the new interference levels can be obtained by simply taking a product of κ_{ij} and the number of users.This simplifies our calculations as the interference need not be recalculated for the new number of users.

Thus, using (2.23) we can compute relative average intercellular interference for an uniform user distribution. Thus, for an uniform user distribution, we can write the total intercellular interference at BS j due to users in cell i as

$$I_{ij} = n_i \times \kappa_{ij} \tag{2.26}$$

It should be noted that the above interference calculations are assuming nominal power as unity. If P is the nominal power from a power controlled user received at home BS, then equation (2.26) would be modified as

$$I_{ij} = P \times n_i \times \kappa_{ij} \tag{2.27}$$

Equation (2.27) gives the total intercellular interference at cell C_j due to users in cell C_i.

2.4 MAI at Home BS

Consider that the desired user is in cell C_i. Hence cell C_i is the home cell, and BS i is the home BS. (refer to Fig. 2.4) The total MAI at home BS has two components; namely

1. Intracell MAI at home BS: $n_i - 1$ users of cell C_i other than the desired user act as interferes. If modeled as a white Gaussian process, its variance $\sigma^2_{I_h}$ can be computed in a way same as (2.15) was derived, giving

$$\sigma^2_{I_h} = \frac{GT_c^2}{6} \sum_{k=1}^{n_i-1} P$$

$$= P(n_i - 1)\frac{GT_c^2}{6} \tag{2.28}$$

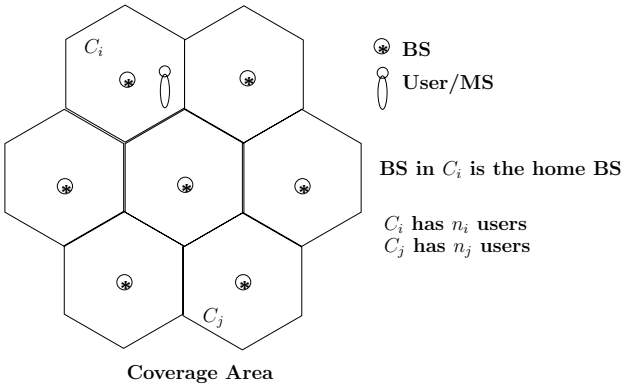

Figure 2.4: Estimation of Total MAI

2. Intercell MAI at home BS: All the users in cells within the coverage area other than cell C_i would contribute to the inter cell interference at BS i. Referring to (2.27), if $\mathcal{A}$ represents the set of cells in the coverage area, then assuming that the nominal power level throughout the coverage area is the same and is P, the total intercellular interference at home BS i , I_{E_h} given by:

$$I_{E_h} = P \sum_{\varphi \in \{\mathcal{A}\}-\{i\}} n_\varphi \kappa_{\varphi i} \tag{2.29}$$

where $\kappa_{\varphi i}$ gives the interference due to a single user in cell φ at BS i, i.e. the home BS.

2.5 MAI at a Non-home BS

For illustration consider that TOA estimation is being carried at BS j, while the user is power controlled by cell C_i. The total MAI at a non-home BS has three components; viz

1. Intracell MAI at BS j: n_j users of cell C_j act as interferes. If modeled as white Gaussian process, its variance $\sigma^2_{I_{nh}}$ is give by

$$\begin{aligned} \sigma^2_{I_{nh}} &= \frac{GT_c^2}{6} \sum_{k=1}^{n_j} P \\ &= P(n_j)\frac{GT_c^2}{6} \end{aligned} \tag{2.30}$$

2. Intercell MAI at BS j due to $N_i - 1$ users of cell C_i: The $n_i - 1$ users of cell C_i other than the desired user act as inter cell interferes to the signal of the desired user at BS j. Referring to (2.27), the total intercellular interference at BS j due to $n_i - 1$ users of cell C_i (home cell) $I_{E_{nh_h}}$ given by:

$$I_{E_{nh_h}} = P(n_i - 1)\kappa_{ij} \tag{2.31}$$

3. Intercell MAI at BS j due to all other cell's: The users of all cells other than cell C_i (home BS) and C_j (cell carrying out TOA estimation) act as inter cell interferes to the signal of the desired user at BS j. Referring to (2.27), the total intercellular interference at BS j due to all other cell's $I_{E_{nh_o}}$ is given by:

$$I_{E_{nh_o}} = P \sum_{\varphi \in \{\mathcal{A}\} - \{ij\}} n_\varphi \kappa_{\varphi j} \tag{2.32}$$

2.6 Signal Strength at the Receiver

In the above sections, we have estimated the total multiple access interference at the BS involved in the process of radiolocation. But, for simulation purpose we also need to consider the attenuation in signal, while it travels from the MS to the receiver. As earlier there are two cases.

1. Signal strength at home BS: As home BS exercises power control over the MS, the power received at the home BS is same as nominal power P. Hence, the received power P_r is given by

$$P_r = P \tag{2.33}$$

2. Signal strength at a non home BS: κ_{ij} gives the interference due to a single user in cell C_i, at BS j. The signal reaching the non home BS j can be considered as interference for the users of cell C_j. It should be noted that κ_{ij} is a measure of power level. For simulations, we need to know the reduction in signal strength, while traveling from a home BS to a non home BS. This is given by $\sqrt{\kappa_{ij}}$. Also, if P represents the nominal received power at a BS, then the signal power received at a non-home BS would be

$$P_r = P\kappa_{ij}. \tag{2.34}$$

Chapter 3

Simulating Subscriber Location

3.1 Tools Used

The following tools were used to develop this simulation

1. Matlab: MATLAB is a high performance language for technical computing. It integrates programming, visualization and computation in a very easy to use environment. Typical uses of MATLAB involve [24]

   (a) Mathematical computation

   (b) Algorithm development

   (c) Modeling, simulation and prototyping

   (d) Data analysis

   (e) Scientific and engineering graphics

   (f) Application development including building of a GUI

   It features a family of add-on application specific packages called 'Toolboxes'. Toolboxes, are a collection of Matlab files (m-files) that extend its functionality to solve a particular class of problem. MATLAB also allows a user to define his own functions and scripts.

   Our simulation uses MATLAB Release 14, V7.0. For application development, we have used the digital signal processing and communications toolboxes.

2. Simulink: Simulink is a software package for modeling, simulating, and analyzing dynamic systems. It supports linear and nonlinear systems, modeled in continuous time, sampled time, or a hybrid of the two. Systems can also be multirate, i.e., have different parts that are sampled or updated at different rates. [25]

   Simulink allows an engineer to move beyond idealized linear models to real world nonlinear, dynamically changing models that describe real world phenomenon. It includes a comprehensive library of sinks, sources, connectors, linear and non-linear components. It

also allows creation of user defined blocks through 'S-Functions'. Functionality can be extended by using application specific blocksets. Simulink also provides various tools for debugging the simulink models.

For our use we have used Simulink 6.0. Our simulation involves use of communication and DSP blocksets.

3. ASAMIN: ASAMIN[26] is a Matlab gateway function to Lester Ingber's "Adaptive Simulated Annealing" (ASA) package.
   ASA [27] is a C-language code developed to statistically find the best global fit of a non-linear constrained non-convex cost-function over a n-dimensional space.
   We estimate the user location by minimizing Equ. (1.12). If we were to minimize it using conventional approaches such as steepest descent algorithms a global optimum may not be obtained. It is also very likely that while searching for an optimal solution, the algorithm gets trapped in local minima's. Functions that have local minima's are called multi-modal functions. Also since the solution space spreads over a large set of points it is very inefficient to exhaustively search for a global minima. To locate minima's for such multi modal functions, the simulated annealing approach is used.
   At the heart, this approach is analogous to thermodynamics [28], specifically the way a liquid freezes and crystallizes, or metals cool and anneal. At higher temperatures, molecules of a liquid move freely, but as the temperature starts dropping, they start coming close to each other and their thermal mobility is lost. As temperature starts dropping, the atoms line up and a crystal is formed that has a very regular structure. Such a state is supposed to be a state of minimum energy. The amazing fact is that for a slowly cooled system, nature is able to find this state of minimum energy, but if the liquid is cooled rapidly or "quenched". It does not reach this state but forms a polycrystalline state or amorphous state having higher energy. Boltzmann (k) distribution given by

$$Prob(E) \approx exp(-\frac{E}{kT}) \tag{3.1}$$

   expresses the idea that a system in thermal equilibrium at temperature T has its energy probabilistically distributed among all different energy states E.
   For minimization of our cost function we have used ASA ver 25.25 obtained from

   `http://www.ingber.com/ASA.zip .`

   As this set of C functions cannot be directly interfaced with Matlab, we have used the ASAMIN package developed by Shinichi Sakata. More detailed information regarding these can be obtained from [27], [28] and [26].

3.2 Components of Simulation

Through our simulations, we have modeled the following components:

1. Coverage area or cell site
2. Position location system

3.2.1 Coverage Area

Coverage area is a simple graphical user interface (GUI), developed in MATLAB, to simulate a CDMA cellular network. It is divided into equal sized grids. User can specify the

1. Length of the coverage area
2. Breadth of the coverage area
3. Width of the grid
4. Breadth of the grid

Figure 3.1 shows a coverage area without any cells in it. An user can place any number of non-

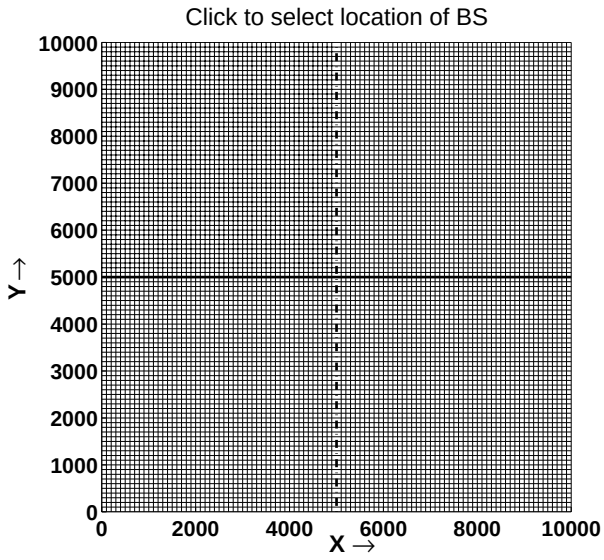

Figure 3.1: Coverage Area

overlapping cells within the coverage area. A cell can be created by clicking anywhere within the coverage area. The point of click specifies the location of the BS for that cell. For creation of a cell, a user needs to specify

- Radius of the cell: The distance between the BS and the farthest point of the cell.
- Transmission power of the BS.
- Number of users in the cell.

- Susceptibility of the cell to fading, in terms of the weight factor α ranging from 0 to 1. As can be seen from Equ. (1.12), a lower value of α_i indicates that results obtained from BS *i* will be weighed less against the results obtained from other BS's. This could be because, BS *i* is prone to heavy losses. For our work, we have assumed α_i=1, i.e. we have weighed every BS equally.

- Shape of the cell: Ideally a cell is visualized as hexagonal in shape, but in practical environments, it is irregular in shape due to the impairments in channels. The tool offers a choice to the users in selecting the cell shape. The cells could be a regular hexagon thus allowing user to tessellate the entire plain without any gaps. Or the cells can be circular such that they completely inscribe the regular hexagon.

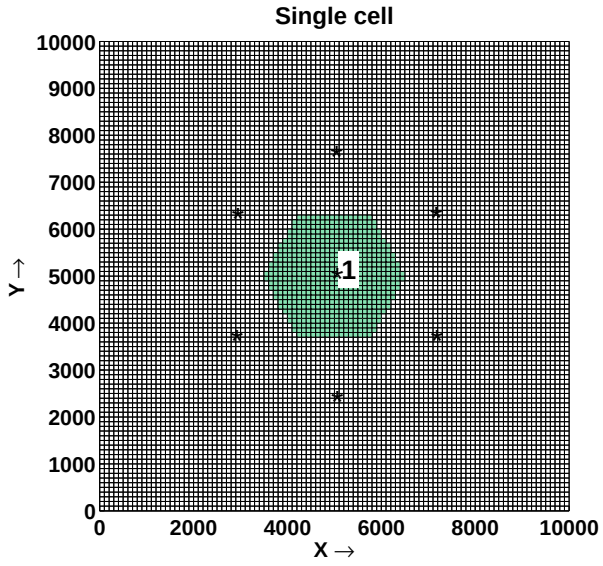

Figure 3.2: A Cell within a Coverage Area

A cell is formed out of a number of smaller grids, as shown in Fig. 3.2. There is no upper limit on the number of cells that can be included in the coverage area. The GUI by itself identifies the location of other BS's so as to minimize inter cellular spaces, based on the data entered for the current cell, and indicates it to the user by means of an '*' on the grid as shown in Fig. 3.2. Figure 3.3 shows a simulated coverage area. The information collected by the GUI is stored in the form of a base station database. A BS database consists of:

Base station ID: An unique number assigned to each base station.

X co-ordinate: X co-ordinate of the base station.

Y co-ordinate: Y co-ordinate of the base station.

Radius: Radius of the cell.

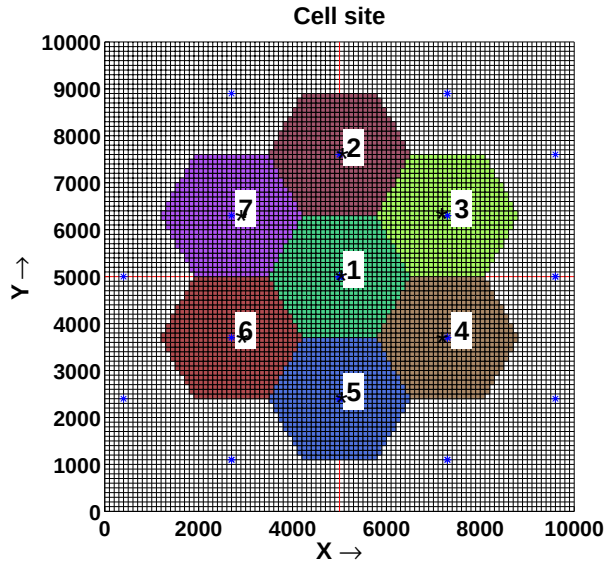

Figure 3.3: Simulated Coverage Area: Hexagonal cells

Cells: Grid points that make up the cell.

Cell shape: Indicates the selected cell shape.

ζ**:** It is the standard deviation of the shadowing losses within a cell.

Along with the above information specific to a base station, the database has the following information needed for the simulation:

Length : The total length of the area in meters.

Breadth : The total breadth of the area in meters.

dx : Horizontal grid size in meters.

dy : Vertical grid size in meters.

cellBinding : It is a boolean variable. It is 0, if we are neglecting shadowing losses within a cell, else it is 1.

F_{ij} **:** It is the interference matrix. If there are N base stations included in the coverage area, F_{ij} is a $N \times N$ matrix, where $f_{ij} \in F_{ij}$ is the interference due to a user in cell C_i at BS j and can be computed using (2.24). But, (2.24) contains an integration over area of a cell, which is difficult to evaluate in MATLAB. Hence we modify (2.24) as

$$\kappa_{ij} = \frac{e^{(\gamma\sigma_s)^2}}{n_i} \sum_{k=1}^{n_i} \frac{d_{ki}^m(x,y)}{d_{kj}^m(x,y)} \tag{3.2}$$

where

- κ_{ij} : It is the value of interference due to a user in cell C_i at BS j.
- n_i : It is the number of grids enclosed within the area defined by cell C_i.
- d_{ki} : It is the distance of the k^{th} grid from the BS of cell C_i.
- d_{kj} : It is the distance of the k^{th} grid from the BS of cell C_j.
- σ_s : It is the standard deviation of the shadowing losses in a cell
- $\gamma : \gamma = \frac{ln10}{10}$.

and evaluate every element of the matrix.

3.2.2 Position Location System

Based on the TOA of the received signal, the position location system attempts to estimate the user location.
Accuracy of estimation depends on:

1. Number of cells within the coverage area.
2. Transmission power of the MS under consideration and other MS within the coverage area.
3. Size of the cells.
4. Number of users in every cell.
5. Number of BS's involved in the process of radiolocation.
6. Characteristics of the TOA estimator.

In our work, we have considered a seven cell system as we are limiting the effect of interference from the first tier of interferer's only. The MS under consideration is under the power control of the central cell so that it finds all the nearest neighbors. To study the effect of MAI on the accuracy of position location, we assume presence of LOS propagation between the MS and BS. This rules out consideration of a microcellular environment. Regarding the cell size, it would be impractical to consider large cells, as large cells require the MS at the cell peripheries to transmit with relatively large powers, while the maximum transmission power from MS is limited by its battery capacity and life. Choosing very small sized cells lead to a microcell environment. Hence cell sizes of 1500m seem to be a good option. We would consider an uniform user distribution.
Figure 3.4 gives a diagrammatic representation of the simulated position location (PL) system. It shows a MS located at (X, Y), whose position is to be estimated. This position in simulation is a random location within the central cell. Now, based on the path loss exponent and shadowing losses the signal undergoes attenuation and reaches the BS's. For improved estimations we need to select the BS's that receive the strongest signals from the MS. The BS's independently estimate the TOA's of the received signals as $\hat{\tau_1}$, $\hat{\tau_2}$ and $\hat{\tau_3}$. After an estimate of TOA's is obtained, the

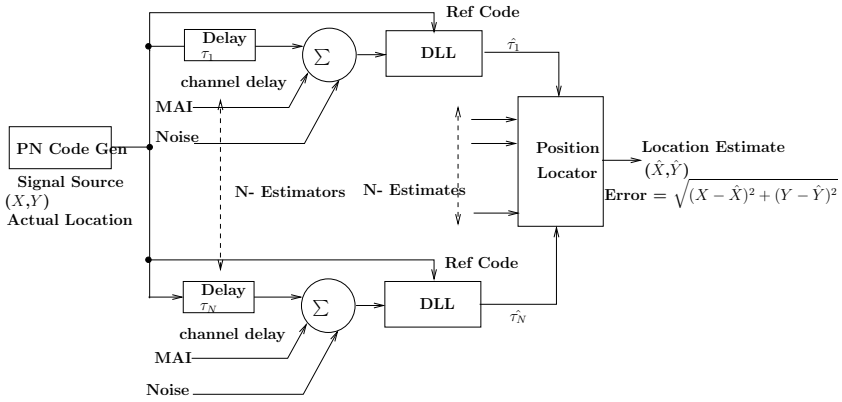

Figure 3.4: Simulated Position Locator System

results are processed by a central processing site and $(\hat{X}, \hat{Y})$ is the estimated location of the MS. The error in estimation is computed as

$$Error = \sqrt{(x-\hat{x})^2 + (y-\hat{y})^2} \tag{3.3}$$

We can list the essential components of the PL system simulation as:

1. Signal generator
2. Channel/Modeling MAI
3. ToA Estimator at the BS
4. Position location (PL) algorithm

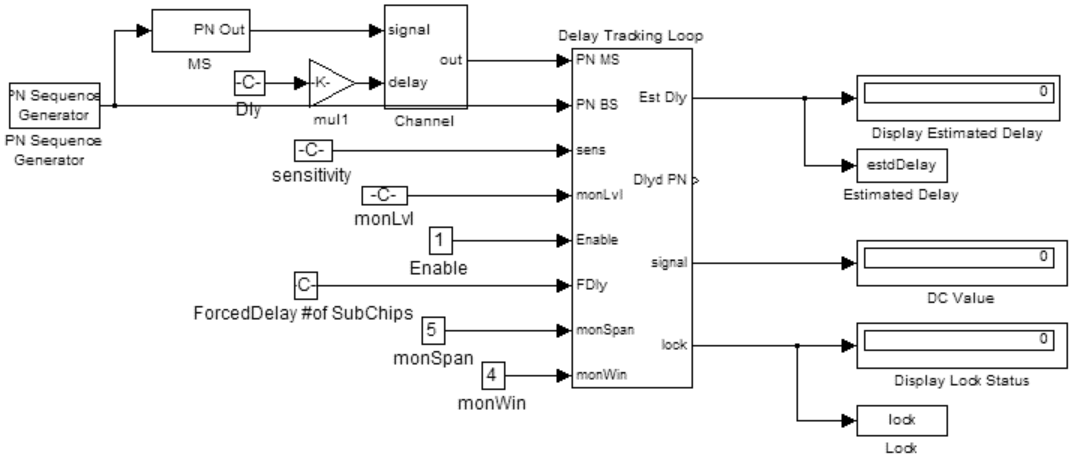

Figure 3.5: Components at the Receiver

We would discuss each of the above in greater detail in the following sections. The Simulated PL system is shown in Fig. 3.5. To simplify the discussion we would begin our discussion with the ToA estimator at the BS, proceed backwards to the MS, and discuss the PL algorithm at the end.

3.2.3 ToA estimator at the BS

ToA estimation is carried out by tracking the received PN sequence. This is accomplished by simulating a non-coherent DLL. A non-coherent loop does not depend on the carrier phase lock, which is difficult to maintain, and hence is less susceptible to lock loss. A conventional non coherent DLL is shown in Fig. 1.11. To study the effect of MAI on accuracy of 2D position location, we assume that the signal transmitted between the MS and BS is a PN sequence. There is no carrier transmitted to the BS. This eliminates the need of the BPF's and squarers shown in Fig. 1.11. The loop filter $F(s)$ shown in the Fig. 1.11 is a LPF for separating the HF components of the received signal. The early and late waveforms are separated from each other by a period equal to $2\Delta T_c$. Δ is the time resolution factor of the DLL and T_c is the chip duration. Δ can take various values such as $\frac{1}{2}$,$\frac{1}{4}$, $\frac{1}{8}$ etc. For example, say $\Delta = \frac{1}{4}$. Then, the early and late waveforms would be separated by $\frac{1}{2}$ a chip period. Lower the value of Δ, better would be the accuracy of estimation. But, the lowest value Δ can achieve is limited by the hardware. Parameter $\frac{1}{\Delta}$ will be referred as sub-chip resolution parameter. Thus, the sub-chip resolution parameter can be defined as the number of intervals in which the tracking loop would divide a single chip interval.
The voltage controlled clock (VCC) source shown in Fig. 1.11, adjusts the phase of the locally generated PN code as per signal $e(t)$. The changes in level of $e(t)$ dictate if the phase of the locally generated PN code has to be advanced or retarded. The simulated version of the DLL is slightly

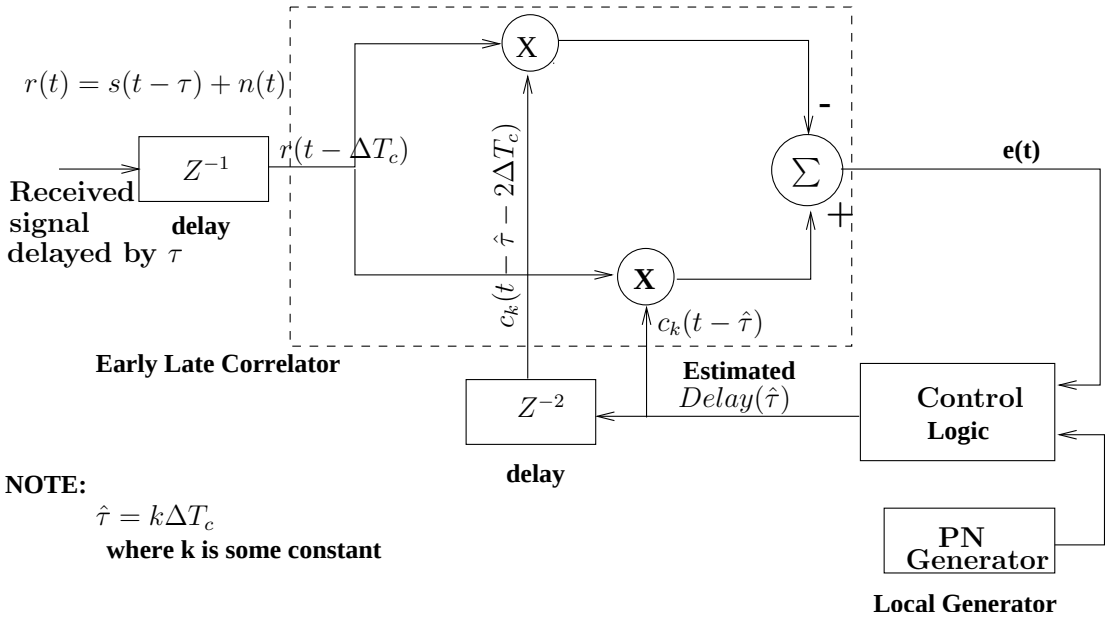

Figure 3.6: Block Diagram of the Simulated DLL

different from the conventional DLL, as discussed above. This difference is due to the limitations of implementation using Simulink. Block diagram of the simulated DLL is shown in Fig. 3.6. The main blocks involved in simulating the DLL are:

Delay elements : An important aspect of simulating the DLL is generating the early and late PN sequences with reference to the locally generated PN sequence. Figure 3.7 shows the

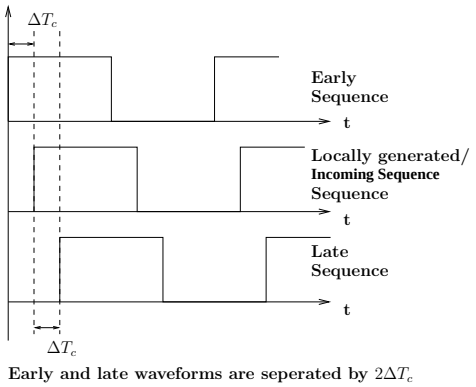

Figure 3.7: Timing Diagram of the Early and Late Sequences

relation of the early and late sequences to the locally generated sequence. It is not possible to generate a sequence ahead of its time. Hence, we cannot derive an early waveform from the locally generated PN sequence. To circumvent this problem, we consider the locally generated PN sequence as reference and use it as an early sequence. The late sequence is derived from the early sequence, by delaying it additionally by $2\Delta T_c$. But, the issue with this approach is that, the incoming sequence and early sequence are no longer separated by ΔT_c. This can be satisfied only if we delay the incoming PN sequence additionally by ΔT_c. With above approach in mind, if the incoming PN sequence is delayed by an amount $k\Delta T_c$ (where k is some constant value), and the ToA estimate achieved using the DLL is also $k\Delta T_c$, then

1. At the input of DLL, the incoming sequence must be additionally delayed by ΔT_c resulting in a total delay of $(k + 1)\Delta T_c$.
2. The early waveform must be delayed by $k\Delta T_c$.
3. The late waveform must be delayed by $(k + 2)\Delta T_c$.

Early-Late correlator : The received PN sequence is multiplied with the locally generated early and late sequences.
Let the received PN sequence be

$$r(t) = s(t - \tau) + n(t),$$

where τ is the delay experienced by the received PN sequence, and

$$s(t) = \sum_{k=-\infty}^{k=\infty} \sqrt{2P_k} C_k(t) \tag{3.4}$$

where $C_k(t)$ represents a PN sequence of k^{th} user of the form [16]

$$c_k(t) = \sum_{j=-\infty}^{\infty} \sum_{i=0}^{M-1} a_{k,i} \Pi(\frac{t-(i+jM)T_c}{T_c}) \qquad (3.5)$$
$$a_{k,i} \in \{-1, 1\}$$

The product results in

$$\begin{array}{lll} Early & product & \sqrt{2P_k}C_k(t-\tau-\Delta T_c) \times C_k(t-\hat{\tau}) \\ Late & product & \sqrt{2P_k}C_k(t-\tau-\Delta T_c) \times C_k(t-\hat{\tau}-2\Delta T_c) \end{array}$$

The resultant signal at the output of early-late correlator is the difference of early and late products given as

$$e(t) = \sqrt{2P_k}C_k(t-\tau-\Delta T_c)[C_k(t-\hat{\tau}) - C_k(t-\hat{\tau}-2\Delta T_c)]$$

where $e(t)$ is called the 'error signal'.
The dc component of $e(t)$ is used for code tracking. The time-varying component is called the 'code self noise'. The dc component of $e(t)$, denoted as $\sqrt{2P_k}D_\Delta(\tau, \hat{\tau})$ is given by:

$$\sqrt{2P_k}D_\Delta(\tau, \hat{\tau}) = \frac{1}{GT_c} \int_{-G\frac{T_c}{2}}^{G\frac{T_c}{2}} e(t)$$

where G is the gain of the CDMA system. Assuming that we are estimating the ToA for user 0,

$$\sqrt{2P_k}D_\Delta(\tau, \hat{\tau}) = \frac{1}{GT_c} \int_{-G\frac{T_c}{2}}^{G\frac{T_c}{2}} \sum_{k=-\infty}^{k=\infty} \sqrt{2P_k}C_k(t-\tau-\Delta T_c)[C_0(t-\hat{\tau}) - C_0(t-\hat{\tau}-2\Delta T_c)]$$

Based on the definition of autocorrelation function of PN sequences, $D_\Delta(\tau, \hat{\tau})$ is defined as

$$\begin{aligned} D_\Delta(\tau, \hat{\tau}) &= R_c(\tau-\hat{\tau}) - R_c(\tau-\hat{\tau}-2\Delta T_c) \\ &= R_c[(\delta)T_c] - R_c[(\delta-2\Delta)T_c] \\ &= D_{2\Delta}(\delta) \end{aligned} \qquad (3.6)$$

This function is plotted in Fig. 3.8 for various values of Δ.

Control logic : The signal e(t) derived from the correlator is fed to a control logic. The role of a voltage controlled clock (VCC) source in the conventional DLL is performed by the control logic in the simulated DLL. Main function of the control logic is to adjust the delay of the early sequence in such a way that it matches with the unknown delay of the incoming PN sequence.

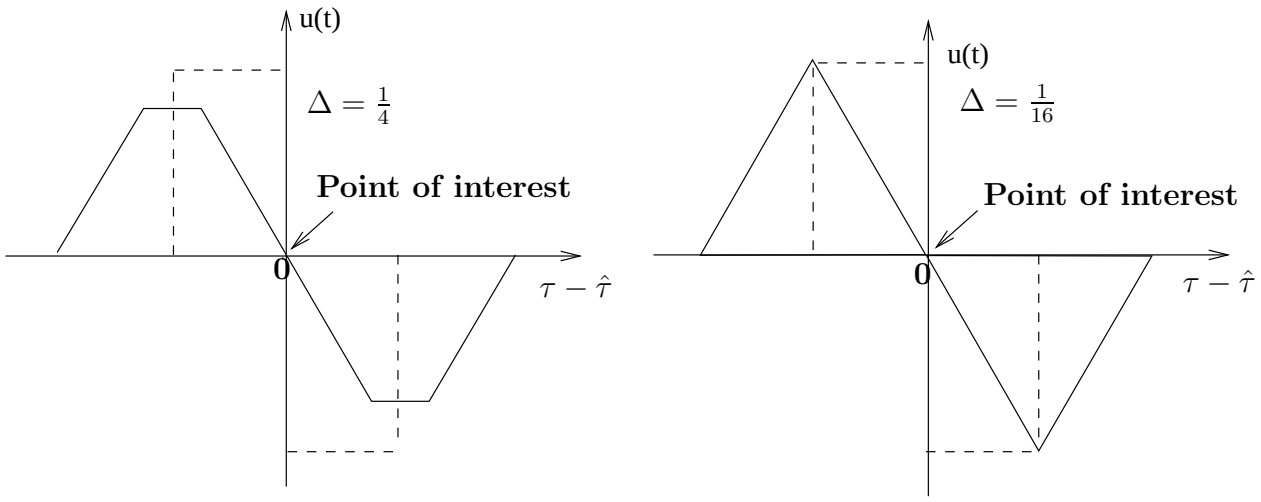

Figure 3.8: S curve's for different values of Δ

Simulated DLL being a discrete system, would alter the delay of early sequence only in steps of ΔT_c. Hence, when the locally generated PN sequence is synchronized with the incoming PN sequence, if the delay suffered by the received sequence is not an integral multiple of ΔT_c, the maximum error in estimation would be $\pm\frac{\Delta T_c}{2}$.
Figure 3.9 shows the simulated tracking loop. Control logic is an 'user defined' Simulink block. The control logic has been implemented as a C-code and then compiled by the MEX compiler to produce the Simulink block. Along with a control unit it consists of a programmable averager. This averager is akin to the integrator employed in a conventional DLL. The time over which it performs averaging can be controlled. Figure 3.10 is the block diagram representation of the integrated control unit. As clearly seen the integrated unit has three sections, namely

1. Averager : This portion acts as an integrator, and computes the average of the error signal arriving within the integration period. The integration period should be long enough to capture the variations in the error signal. Ideally it is set to G chip periods, where G is the gain of the CDMA system. The averaging operation can be understood as a reset able accumulator followed by a scaling operation.The time of integration is an user defined parameter in the simulations, and can be altered. Internally the control unit counts the number of samples. If T_{int} represents the value of integration period, then for zero delay, the control unit accepts $\frac{T_{int}}{\Delta}$ number of samples and computes its mean. For delay's > 0, the control unit automatically expands the integration period by a value $\frac{\hat{\tau}}{\Delta}$, where $\hat{\tau}$ represents the estimated delay value. This is done to compensate for the additional bits inserted by the delay blocks. For further discussion, we would represent the computed average value as $S_{\hat{\tau}}$.

2. Running sum: Figure 3.8 shows the early-late discriminator characteristics. Estimation is exact at the point where the S-curve crosses the zero level. But, in noisy environments, as shown in 3.11, it is difficult to estimate the point where it crosses the zero level. A complex

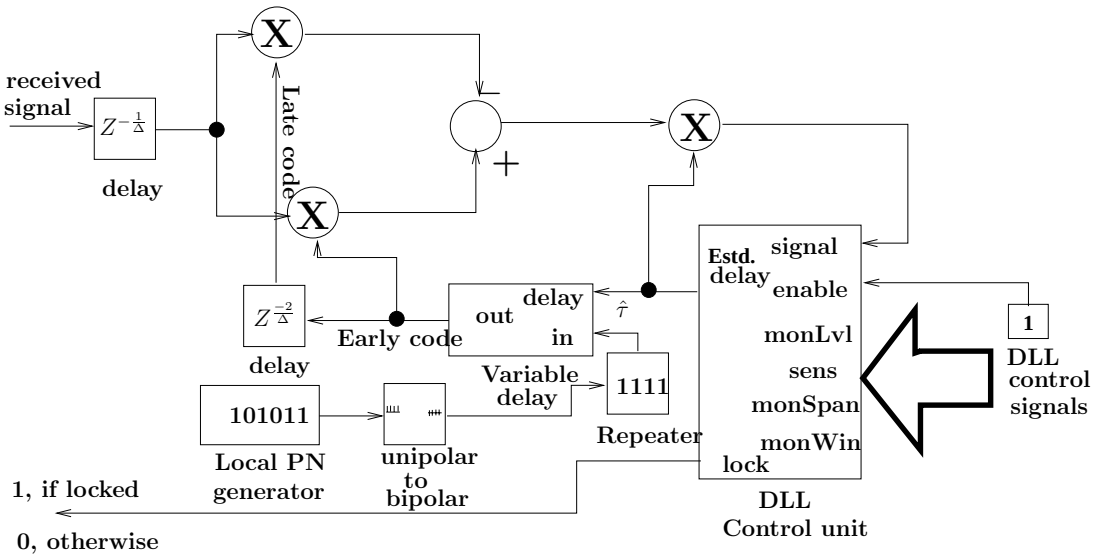

Figure 3.9: Functional Diagram of the Simulink Model of Tracking Loop

algorithm should be used to detect the point of interest. To circumvent this, we employ a running sum over the error signal. Advantage of doing so is obtained in terms of reduction of number of zero crossing points. The characteristics are transformed from a S-shaped curve to an inverted V-shaped curve as shown in Fig. 3.12. Characteristics shown in Fig. 3.12, for different values of Δ, were obtained at the time of simulation at a home BS for SNR=25dB.

In the transformed characteristics, a match is found when the curve attains a peak, which is well defined. Also, in the case of noisy environments, the detection would be simpler and results would be more accurate as peak will be well above the noise floor.

The control unit, internally keeps on adding the $S_{\hat{\tau}}$'s, and this operation is called running sum operation.

3. Control unit : Figure 3.12 shows the discriminator characteristics for various values of Δ. Primary function of the control unit is to detect the peak. For detection of the peak, we use the 'serial search technique' [22]. It employs searching serially through all potential code delays until the correct delay is identified. Each estimated delay is evaluated by an attempt to despread the received signal. If the estimated delay is correct, the received signal will be despread and will be sensed. If the estimated delay is incorrect, the received signal will not be despread and the delay of the reference code will be stepped to a new value of delay. This technique is called the 'serial search'.

   The basic principle of working of the serial search technique, is the fact that an appreciable signal level will be produced by the discriminator when the locally generated sequence despreads the received signal. Similar is the working principle of the control unit. It keeps on delaying the locally generated PN sequence until it senses an appreciable level of the

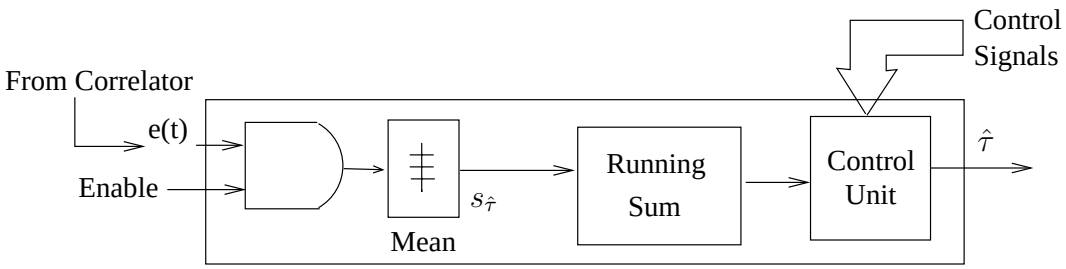

Note:
$\hat{\tau}$ => Estimated Delay

Figure 3.10: Block Diagram of the Control unit

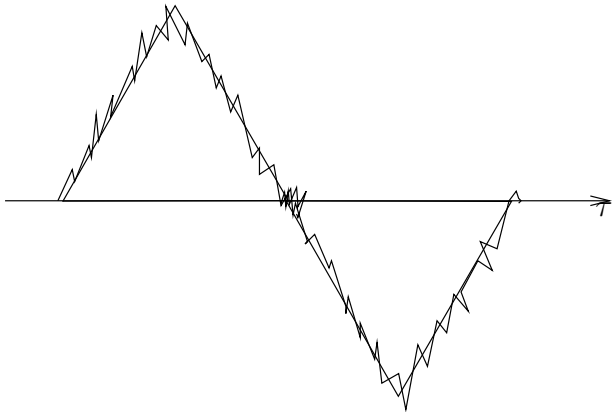

Figure 3.11: Discriminator Characteristics under Noisy Conditions

despread signal. The discriminator characteristics shown in Fig. 3.12 are plotted when the SNR of the received signal is very high. But, in practical scenarios, the actual SNR levels can be lower than 0dB at non-home BS's. Thus, a more realistic discriminator characteristic is shown in Fig. 3.13. The figure shows more than one peak, and hence it is difficult to determine the exact value of delay that would despread the received signal. A control unit must be intelligent enough to disregard the false alarms triggered by the noisy error signal. This intelligence is engineered in the control unit by means of some control signals. The following describes each of the control signals in detail.

(a) sens : It stands for the sensitivity of the control unit. Suppose it is set to 10^{-3}, the control unit would not respond to signal variations less than, 10^{-3}. Thus, it prevents DLL from responding to small variations in the error signal.

(b) monLevel : It stands for 'monitor level'. As can be seen from Fig. 3.13 this serves as a reference level to the control unit. Only when, accumulated value of the signal $S_{\hat{\tau}}$, crosses the reference level, the control unit starts a serial hunt for the peak.

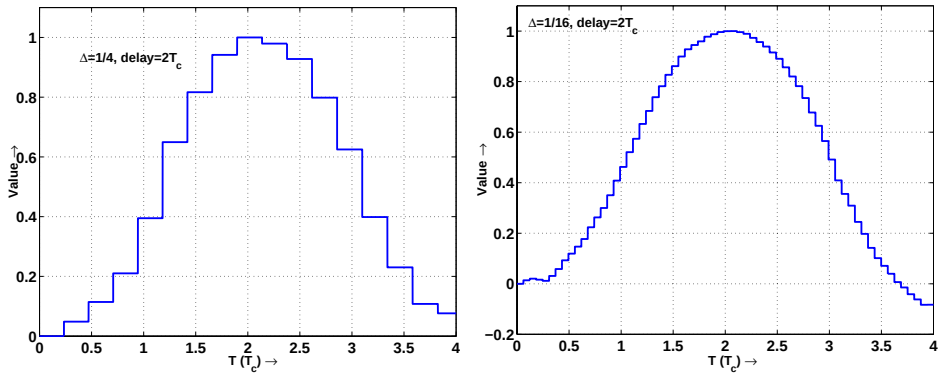

Figure 3.12: V curve's for different values of Δ

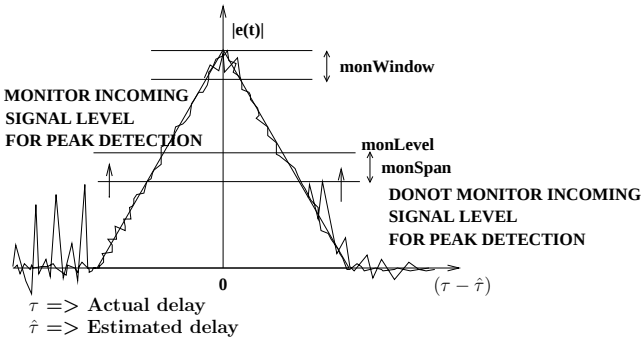

Figure 3.13: Control Signals used by the Control Unit

(c) monSpan : It stands for 'monitor span'. Because of the addition of variable amount of noise, it is not always possible to define a discrete monitor level. Hence, optionally a provision is made in terms of the control signal *monS pan* that reduces the monLevel to $monLevel - \frac{monS\ pan \times monLevel}{100}$. An alternative could be setting the *monLevel* to lower value, and *monS pan* to zero.

(d) monWindow : It stands for 'monitor Window'. The basic principle of operation of the control unit is to serially search for the peak and delay the locally generated PN code until an appreciable signal level is detected. But, it is very much possible that once a peak is attained, the signal level momentarily drops due to the noisy signal and attains a higher peak level after recovering from a momentary fade. To tackle this situation, we allow the signal level to drop within *monWindow* percent of the attained level, before it concludes that the current level is the peak level. If the signal level falls more than that, it is concluded that we just crossed the peak and the peak hunting stops.

It should be noted that, the peak level is not defined. It is any level above the monitor level. But in practice, it is very likely that the received signal never crosses the monitor level. This can happen when the signals are weak. To handle such situations, the control logic

is defined in such a way that, if during its exhaustive search it hits the maximum possible trackable delay, it sets the estimated delay to a value of delay $\hat{\tau}$, for which it encountered the maximum value of $S_{\hat{\tau}}$. The maximum track able delay is defined as '*maxDelay*'.

Depending on the error signal $e(t)$, the control block would produce a value $k\Delta$ by which the early sequence is delayed. Since $0 \leq \Delta \leq 1$, it is difficult in Matlab to delay the sequences by fractional values, so we expand all the sequences by a factor $\frac{1}{\Delta}$ and delay the early sequence by k. Hence the locally generated PN sequence is expanded by a factor $\frac{1}{\Delta}$ using the repeater block from the DSP blockset. The control logic is modified to produce an output k instead of $k\Delta$.
In an actual DLL, the loop filter consists of an integrator, that integrates the incoming signal for a specified time. In the simulated DLL, the integrator is embedded within the control block. The duration of integration is specified by the parameter 'clkPeriod'. Ideally, integration is carried over a bit interval. Hence *clkPeriod* is set to a value same as the gain of CDMA system G. For our simulations, value of this variable is set to 128.

3.2.4 Channel

We model the MAI at each BS by a white Gaussian noise process. In light of the central limit theorem and with large number of interferer's this modeling assumption is justified. It is necessary that the power of this WGN added at the BS is derived from the amount of MAI the signal would experience. As explained earlier, the total interference at a home BS is different from the total interference at a non-home BS. Similarly, the amount of WGN to be added at a home BS will be different from the WGN added at a non-home BS.

3.2.4.1 Total Noise due to MAI at the Receiver Input at Home BS

For a home cell, equation (2.17) gives the variance of the total noise (excluding intercellular noise) present at the output of a decorrelator (despreader) and demodulator. In our simulations the MAI is modeled as a white Gaussian process at the output of receiver. Thus, the variance of this process needs to be recalculated so as to represent the same variance σ_ζ^2 at the output of the despreader and the demodulator. Thus, if $\sigma_{I_h}^2$ represents the variance of intracellular multiple access interference at the receiver input,
from calculations similar to that leading to equation (2.14) we get

$$\sigma_\zeta^2 = \sigma_{I_h}^2 \frac{T_b}{2} \tag{3.7}$$

Thus,

$$\begin{aligned}\sigma^2_{I_h} &= \sigma^2_\zeta \frac{2}{T_b} \\ &= G\frac{T_c^2}{3T_b}(n_i - 1)P \\ &= G\frac{T_c^2}{3GT_c}(n_i - 1)P \\ &= \frac{T_c}{3}(n_i - 1)P \end{aligned} \tag{3.8}$$

Let W denote the chip rate. Then 3.8 can be rewritten as

$$\sigma^2_{I_h} = \frac{1}{3W}(n_i - 1)P \tag{3.9}$$

Thus, total intracellular multiple access interference at the receiver input can be modeled as white Gaussian noise process with variance $\sigma^2_{I_h}$ given by equation (3.9).
The total intercellular interference at a home BS i, as derived in section 2.4 is given by (2.29) as

$$I_{E_h} = P \sum_{\varphi \in \{\mathcal{A}\} - \{i\}} n_\varphi \kappa_{\varphi i}.$$

Equation (2.29) gives the total interfering power at home BS i. Note that the interference I_{E_h} as calculated in (2.29) is at the input of the decorrelator. Thus after decorrelation and demodulation the variance of the WGN modeling the intercell MAI will be equal to the PSD of the intercell interference, given by

$$\begin{aligned}\sigma^2_{E_h} &= \frac{I_{E_h}}{W} \\ &= \frac{P}{W} \sum_{\varphi \in \{\mathcal{A}\} - \{i\}} n_\varphi \kappa_{\varphi i}. \end{aligned} \tag{3.10}$$

Thus, the variance of the modeled noise due to MAI at the receiver input at home BS is given by

$$\begin{aligned}\sigma^2_h &= \sigma^2_{I_h} + \sigma^2_{E_h} \\ &= \frac{1}{3W} \sum_{k=1}^{n_i - 1} P + \frac{P}{W} \sum_{\varphi \in \{\mathcal{A}\} - \{i\}} n_\varphi \kappa_{\varphi i}. \end{aligned} \tag{3.11}$$

3.2.4.2 Total Noise due to MAI at the Receiver Input at a Non-Home BS

As explained in section 2.5, total MAI at a non-home BS is made up of three parts

1. Intracell interference due n_j users of the non-home BS j, given by (2.30) as

$$\sigma^2_{I_{nh}} = \frac{GT_c^2}{6}\sum_{k=1}^{n_j} P$$
$$= Pn_j\frac{GT_c^2}{6}$$

2. Intercell interference due to $n_i - 1$ users of the home BS i, given by (2.31) as

$$I_{E_{nh_h}} = P(n_i - 1)\kappa_{ij}$$

3. Intercell interference due to users of all other cells, given by (2.31) as

$$I_{E_{nh_o}} = P\sum_{\varphi\in\{\mathcal{A}\}-\{i,j\}} n_\varphi\kappa_{\varphi j}$$

The total interference at the input of receiver is the sum of all the above interferences. Thus, it is merely the sum of all the interfering powers and hence can be modeled as WGN, as explained in section 2.4. Thus, the variance of the modeled WGN at the input of receiver at a non-home BS is given as

$$\begin{aligned}\sigma^2_{nh} &= \sigma^2_{I_{nh}} + \sigma^2_{E_{nh_h}} + \sigma^2_{E_{nh_o}} \\ &= \frac{P}{3W}n_j + \frac{P}{W}(n_i - 1)\kappa_{ij} + \frac{P}{W}\sum_{\varphi\in\{\mathcal{A}\}-\{i,j\}} n_\varphi\kappa_{\varphi j}\end{aligned} \tag{3.12}$$

Figure 3.14 shows the SIMULINK implementation of the channel discussed above. The blocks

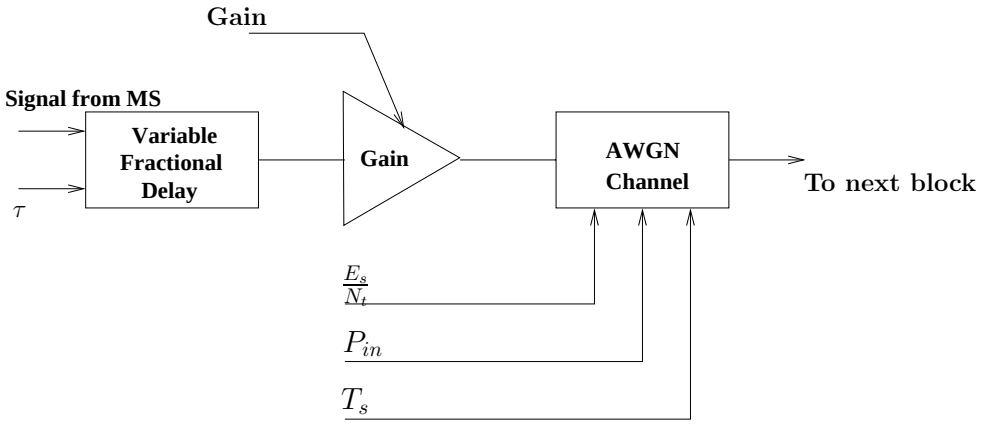

Figure 3.14: Model of a Radio Channel in Simulation

used to simulate the channel are:

1. AWGN channel: This block adds white Gaussian noise to the input signal. The variance of the noise is specified in terms of

   - $\frac{E_s}{N_t}(dB)$: It is the ratio of signal energy to noise power spectral density in dB. Equations (2.33) and (2.34) give the power received at home and non-home BS's respectively. If T_b denotes bit period, the total signal energy over a bit duration at a home BS is given by:

     $$E_s = P \times T_b. \tag{3.13}$$

     Similarly, the total signal energy over a bit duration at a non-home BS is given by:

     $$E_s = P\kappa_{ij} \times T_b. \tag{3.14}$$

     For IS-95 CDMA standard, full rate bit rate is 9600bps and hence T_b is 10.416mSec. The PSD of noise due to MAI at the receiver input is given by (3.11) and (3.12). The total noise at a receiver input would include thermal noise in addition to the MAI given by (3.11) and (3.12). If $\frac{N_0}{2}$ represents the PSD of thermal noise at the receiver input, the total noise PSD at the receiver input of a

     – Home BS is given as:

       $$N_t = \sigma_h^2 + \frac{N_0}{2}$$

       using (3.11), we obtain

       $$N_t = \frac{1}{3W}\sum_{k=1}^{n_p-1} P + \frac{P}{W}\sum_{\varphi\in\{\mathcal{A}\}-\{i\}} n_\varphi \kappa_{\varphi i} + \frac{N_0}{2} \tag{3.15}$$

     – Non-home BS is given as:

       $$N_t = \sigma_{nh}^2 + \frac{N_0}{2}$$

       using (3.12), we obtain

       $$N_t = \frac{P}{3W}(n_j) + \frac{P}{W}(n_i - 1)\kappa_{ij} + \frac{P}{W}\sum_{\varphi\in\{\mathcal{A}\}-\{ij\}} n_\varphi \kappa_{\varphi j} + \frac{N_0}{2} \tag{3.16}$$

     In our simulations we have added $10^{-8} watt/Hz$ of thermal noise. Hence,

     $$\frac{N_0}{2} = 10^{-8} \tag{3.17}$$

     Thus, signal energy to noise power spectral density in dB can be computed as

     $$\frac{E_s}{N_t}(dB) = 10\log\frac{E_s}{N_t}, \tag{3.18}$$

     where, for a home BS E_s and N_t are given by (3.13) and (3.15) respectively, while for a non-home BS's they are given by (3.14) and (3.16) respectively.

- Power P_{in}: It is the power received at a BS and is given by (2.33) and (2.34) for home BS and non-home BS's respectively.
- Symbol period T_s: We assume, the use of a modulation scheme where the symbol duration is same as bit duration, and hence $T_s = T_b$.

2. Gain: As discussed in section 2.6, signal suffers attenuation while traveling from a MS to a BS. It is necessary to model this attenuation while simulating a position location system. Using (2.33) and (2.34) if the MS is power controlled by C_i and we are estimating the ToA at BS j, we get

$$Attenuation = \begin{cases} 1 & i = j \\ \sqrt{\kappa_{ij}} & i \neq j \end{cases} \tag{3.19}$$

   To model the attenuation, we scale the incoming signal using the 'Gain' block with the scaling factor set to the desired value of attenuation.

3. Variable fractional delay: When signal transmitted from a MS at (x, y) reaches a BS at (x_i, y_i) it travels a distance d given by

$$d = \sqrt{(x - x_i)^2 + (y - y_i)^2}$$

   If c denotes the velocity of light, the time taken by the signal to reach the BS, assuming absence of multipath propagation, is given as $\tau = cd$. This block is used to model this delay τ. Any signal transmitted from MS is delayed by a time equal to τ.

3.2.5 Signal Generator

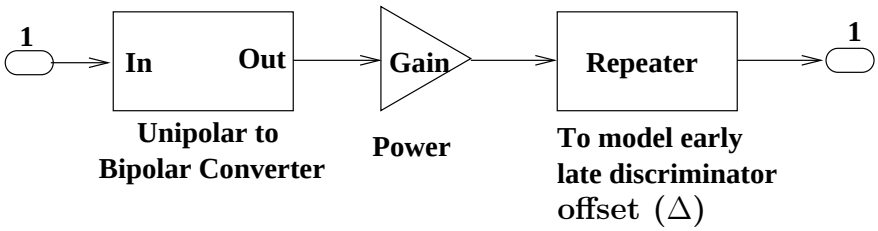

Figure 3.15: Model of a Signal Generator in Simulation

It represents the signal generator (MS) whose location is to be estimated. It is made up of the following blocks from the SIMULINK library:

- Unipolar to bipolar converter: In practice, the PN sequences employed over CDMA networks are bipolar in nature. Hence, in our simulations we convert the unipolar PN sequences to bipolar. This block takes input from a PN sequence generator and converts it to a signal with levels ±1.

- Gain: If P_{nom} is the received signal power at a home BS, then using (2.1) we conclude that the signal amplitude is $\sqrt{2P_{nom}}$. Hence, we need to scale the signal with level ± 1 to $\pm\sqrt{2P_{nom}}$. This is done using the 'gain' block from the Simulink library.

- Repeater: It up-samples the input, to a rate L times higher than the input sample rate by repeating each consecutive input sample L times at the output. The Repetition count parameter L is the value of $\frac{1}{\Delta}$.

3.2.6 Position Location (PL) Algorithm

As discussed in 1.3.3, the method of non Linear Least Squares (NLLS) is a very popular method of deriving position estimate using the estimated ToA's. We need to minimize the cost function in (1.12) given as

$$F(\mathbf{z}) = \sum_{i=1}^{N} \alpha_i^2 f_i^2(x).$$

One method of optimization is the method of steepest descent [1]. But, the method of minimiza-

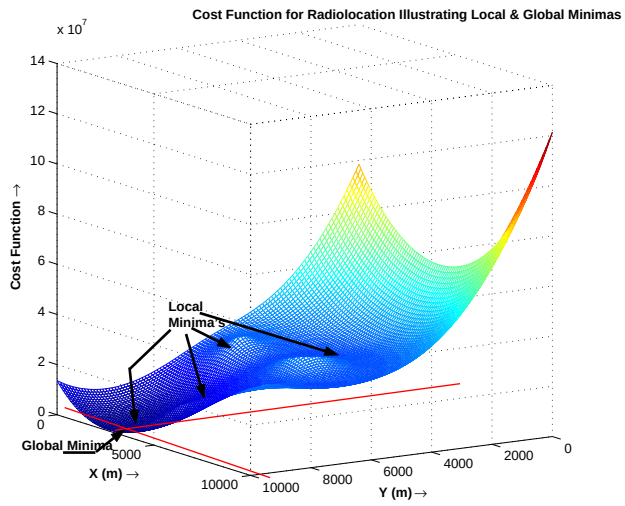

Figure 3.16: Plot of Cost Function $F(\mathbf{z})$

tion using the method of steepest descent has the following drawbacks:

Convergence A typical plot of the cost function (1.12) is shown in Fig.3.16. As the cost function is not a convex function, steepest descent may get stuck in a local minima and result in a sub optimal solution.

Slow rate of convergence It could take very long before the minimization algorithms converge to produce an optimal result.

To overcome the inaccuracies in position estimation due to optimality in convergence and to reduce the convergence time, we have used the method of 'Simulated Annealing' [27].
We have integrated MATLAB with the simulated annealing package using ASAMIN. More on the ways of integration can be read from [26].
To communicate the results of ToA estimations to ASAMIN, we need to form the cost function $F(\mathbf{z})$. The Matlab version of the cost function is as follows:

```
function [cost_value, cost_flag] = test_cost_func1 (param)
%
%  $Id: costFunc.m    $
%
1>   global alpha;    %Weight Vector
2>   global EstdDELAY;   %Estimated Delay  Vector
3>   global XI;        %Vector containing the X Co-ordinate of the BS's involved in ra
4>   global YI;        %Vector containing the Y Co-ordinate of the BS's involved in ra
5>
6>   c=3*(10^8);     % velocity of light
7>   f=(c.*EstdDELAY)-sqrt(((XI-param(1)).^2)+((YI-param(2)).^2));
8>   F=sum((alpha.^2).*(f.^2));
9>   cost_value = F;
10> cost_flag=1;
11> if(cost_value<0)
12>    cost_flag=0;
13> end;
```

A terminating condition is very essential while defining any minimization maximization algorithm. $F(\mathbf{z})$ being a sum of squares should always be positive. Hence, the minimum value, it could attain would be zero.
Variables

```
cost_value, cost_flag
```

are reserved by the ASAMIN package and posses special meanings. In line 9, it is indicated to ASAMIN that our cost function is defined by F. Lines 11-13 test for the terminating condition. If the value of cost function becomes negative, the variable

```
cost_flag
```

is set to zero, that is an indication to ASAMIN to terminate the process.
Once the algorithm converges, it returns the estimated values $(\hat{x}, \hat{y})$ of MS location.

3.3 Software Flowchart

Figure 3.17 presents an overview of the program used to estimate user location in CDMA network. Using the base station database, and the values of

P_{nom} **:** Nominal power of the received signal at a home base station.

$ChipRate, R_c$ **:** The chip rate.

Bit rate: This is the rate of the channel. Currently we have fixed it to 9600bps.

num_{user} **:** The number of users in every cell.

σ_s **:** The standard deviation of shadowing losses in every cell.

num_{BS} **:** This is the number of BS's participating in the triangulation process.

subChip : This reflects the time tracking capability of the DLL.

$T_{integrate}$ **:** It sets the time of integrator in the DLL.

the entire simulation is carried out.

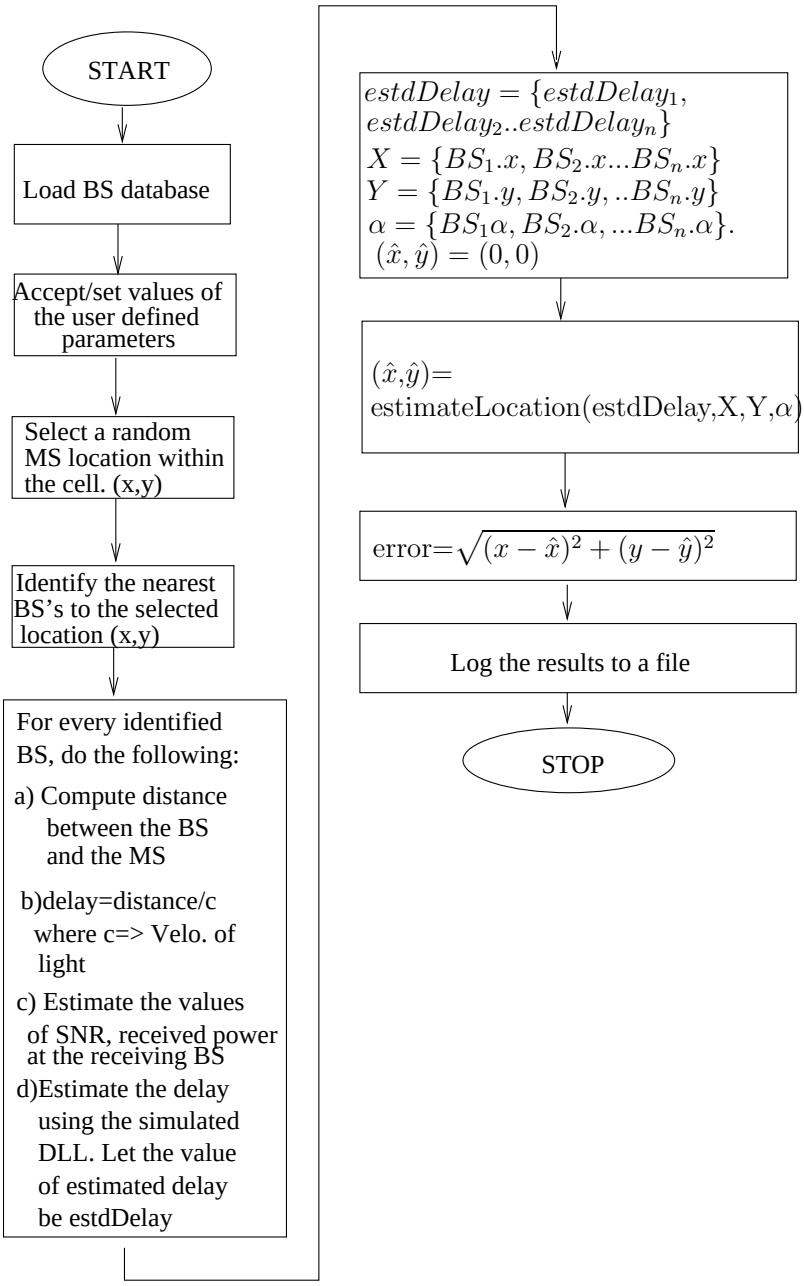

Figure 3.17: Flowchart of the Position Estimation Software

Chapter 4

Results

To study the effect of MAI on the estimation error, simulation experiments were carried out with the following set of fixed parameters:

1. As per IS-95 standards, a chip rate of 1.2288MHz was selected. Hence, Rc = 1.2288 Mcps.
2. As per IS-95 standards, gain of the CDMA system is 128. Hence, G=128
3. For most practical purposes, path loss exponent for mobile communications is 4 [23]. Hence, m=4
4. As we are restricting the interference from the first tier of interferer's, number of cells in the coverage area is 7. Hence, $NBS = 7$
5. The value of α for home BS is unity.
6. The value of α for non-home BS is 0.3.
7. Nominal power of MS, $P_k = 1$
8. Speed of radio signal, C = 3x10^8 m/Sec
9. Thermal noise, $\frac{N_0}{2} = 10^{-8}$ dB/W
10. User distribution per cell is uniform and every cell has same number of users N.

The variable set of parameters included:

1. N: Number of users per cell.
2. σ_s: The standard deviation of shadowing losses in every cell.
3. N_{BS}: Number of BS's participating in radiolocation.
4. Δ: DLL resolution.
5. R: Radius of the cells.

Through our experiments, we have studied the:

Table 4.1: List of Experiments

σ_s (dB)	N	N_{BS}	Δ	R
6	1 to 100 in steps of 10	3	$\frac{1}{8}$	$1500m$
8	1 to 100 in steps of 10	2	$\frac{1}{8}$	$1500m$
8	1 to 100 in steps of 10	3	$\frac{1}{8}$	$1500m$
8	1 to 100 in steps of 10	4	$\frac{1}{8}$	$1500m$
8	1 to 100 in steps of 10	3	$\frac{1}{2}$	$1500m$
8	1 to 100 in steps of 10	3	$\frac{1}{4}$	$1500m$
8	1 to 100 in steps of 10	3	$\frac{1}{8}$	$100m$
8	1 to 100 in steps of 10	3	$\frac{1}{8}$	$500m$
10	1 to 100 in steps of 10	3	$\frac{1}{8}$	$1500m$

1. Effect of varying the number of users per cell, assuming an uniform distribution,on the accuracy of estimation.
2. Effect of varying shadow losses on the accuracy of estimation.
3. Effect of varying the number of BS's participating in radiolocation on the accuracy of estimation.
4. Effect of varying the DLL resolution on the accuracy of estimation.
5. Effect of varying the size of cells on the accuracy of estimation.

The set of experiments carried out are listed in table 4.1.
Some other notations used in the explanation ahead are:

N_{BS} **:** It represents the number of BS's used for radiolocation.

T_{int} **:** It represents the integration period of the control unit.

4.1 Effect of Varying Shadowing Losses on the Accuracy of Radiolocation

This experiment was conducted to study the combined effect of varying shadowing losses and the number of users per cell on the error in radiolocation. To carry out the experiment:

1. Set
   - $\Delta=\frac{1}{8}$.
   - Number of BS's participating in radiolocation = 3.

- Radius of the cell = 1500m.
- Integration period = $T_{int} = 128T_c$.

Generate a cell site BS database for 7 cells of radius 1500m each, using the GUI. Set value of σ_s to 6dB.

2. For the given value of σ_s compute the interference matrix F_{ij}.
3. Now, vary the number of users per cell from 1 to 100, in steps of 10, and estimate the error in position estimation as per Fig. 3.17.
4. Similarly, set σ_s=8dB and 10dB, and goto step 2.

For every setting of σ_s, and number of users per cell, 50 random locations were chosen within the central cell, and estimations were carried out. The final results are an average of the results obtained at the 50 locations. Similar procedure is carried out for the remaining set of experiments. Variation in shadowing losses will have a considerable effect on the SNR at the receiving BS's. Figure 4.1 shows the variation in SNR at a home BS with the number of users per cell N, and σ_s.

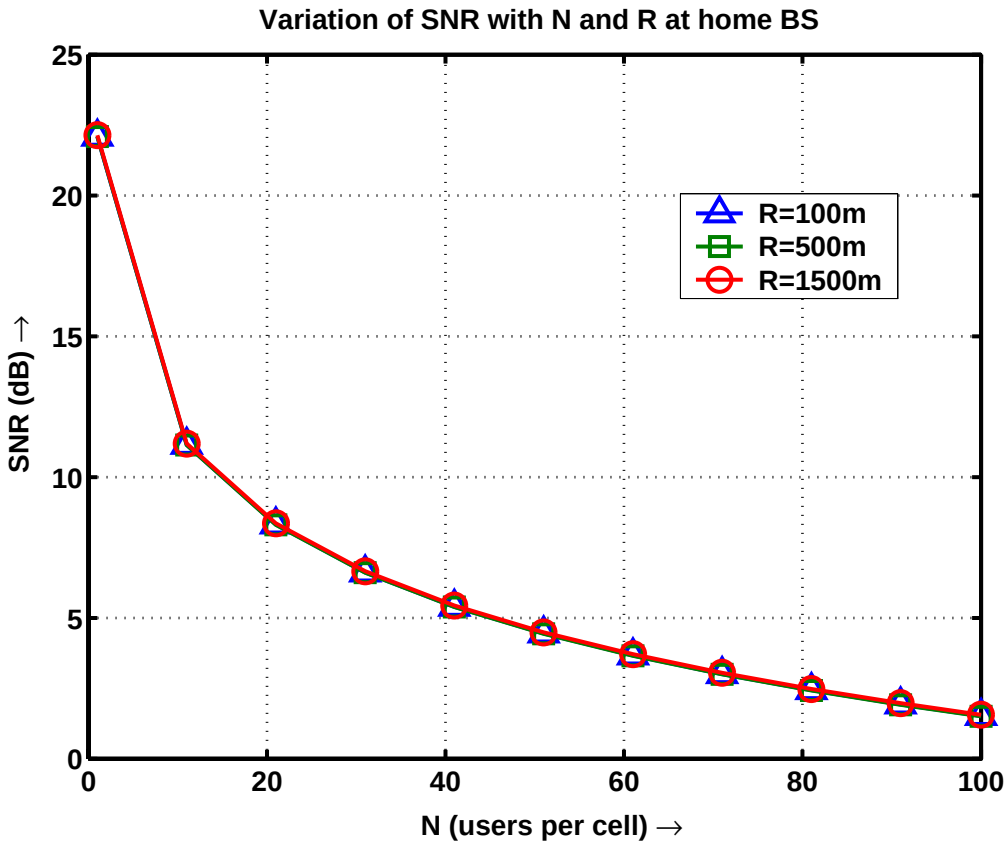

Figure 4.1: Measured SNR at Home BS

The following conclusions can be drawn from Fig. 4.1.

1. **For a given value of σ_s, SNR decreases as N increase:** Equation (3.11) gives the total interference at a home BS for a given number of users in a cell. The total amount of interference is proportional to the number of users in the cell. Thus, as the number of users per cell increases, the total interference at a home BS increases, thereby degrading the SNR.

2. **For a given value of N, SNR decreases as σ_s increases:** From (3.11) and (2.24), we can say that for a given number of users per cell, the total interference increases with the σ_s, standard deviation of shadowing.

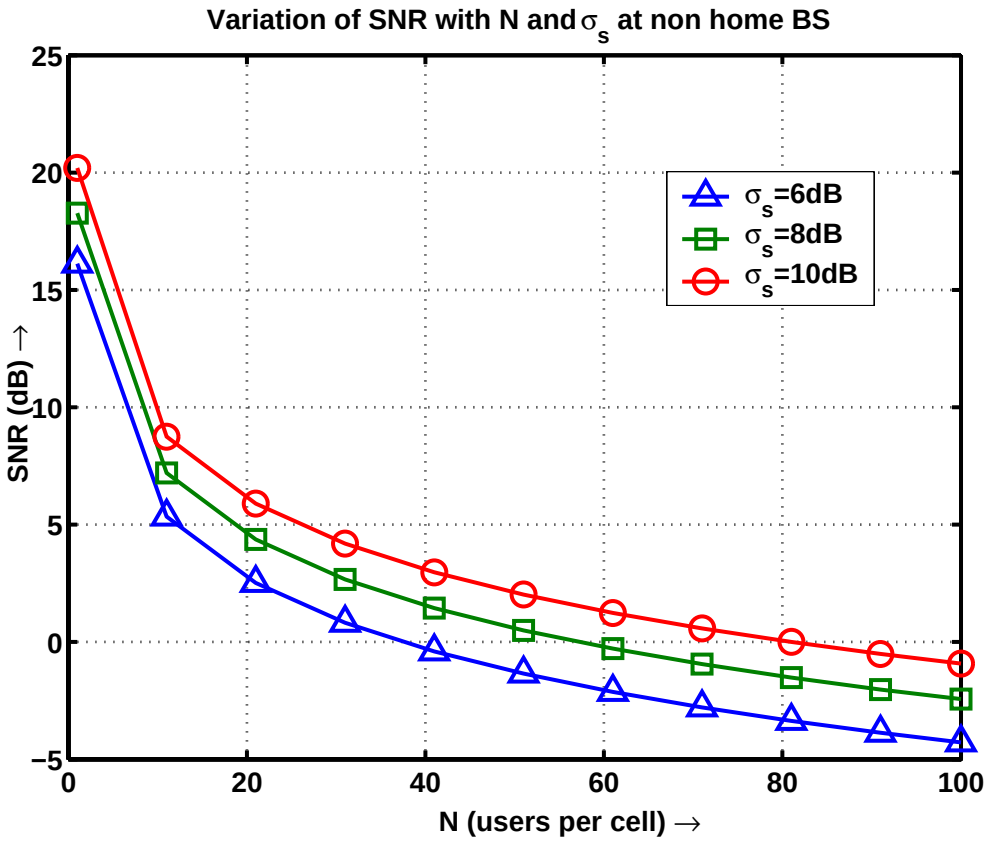

Figure 4.2: Measured SNR at Non-Home BS

Figure 4.2 shows:

1. **At a non-home BS, for a given value of σ_s, SNR decreases as N increase:** Equation (3.12) gives the total interference at a non-home BS for a given number of users per cell. The total amount of interference at a non-home BS is proportional to the number of users per cell. Hence, as the number of users per cell increases, the total interference at a non-home BS increases, thereby degrading the SNR.

2. **For a given value of N, SNR increases as σ_s increases:** From (3.12) and (2.24), we can say that for a given number of users per cell, the total interference increases exponentially as the standard deviation of shadowing, σ_s. For a given number of users, the interference increases as the value of σ_s. But, SNR is a ratio of the received signal energy and the interfering power. The received signal strength at a non-home BS depends on the value of κ_{ij} given by Equ. (2.34). κ_{ij} increases exponentially with σ_s. As the value of σ_s increases, due to perfect power control, the transmitting power of a MS increases, thus increasing the energy of the signal reaching the non-home BS. SNR at a non-home BS is the ratio of two terms, with denominator having a term independent of σ_s. Hence, numerator varies faster than the denominator which leads to an increase in the received SNR at a non-home BS with σ_s.

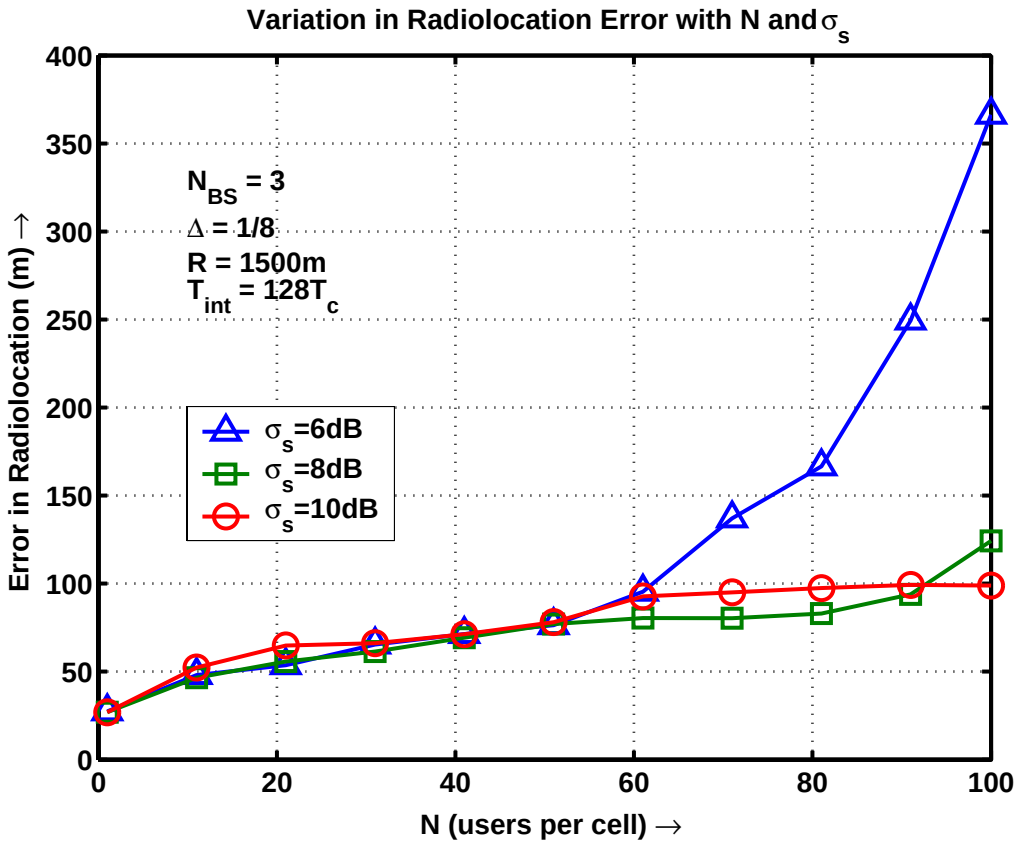

Figure 4.3: Variation of Radiolocation Error with N and σ_s

The plot in Fig. 4.3 shows the variation of error in radiolocation with number of users per cell and σ_s. The mean value of the radiolocation error, tabulated below is determined by taking an average of all the points plotted in the Fig. 4.3. When the number of users are varied from 1 to 100, other conditions remaining same, the minimum, maximum and mean values of the observed errors are tabulated in Table 4.2. Plots in Fig. 4.4 reveal that the ToA estimation at a home BS

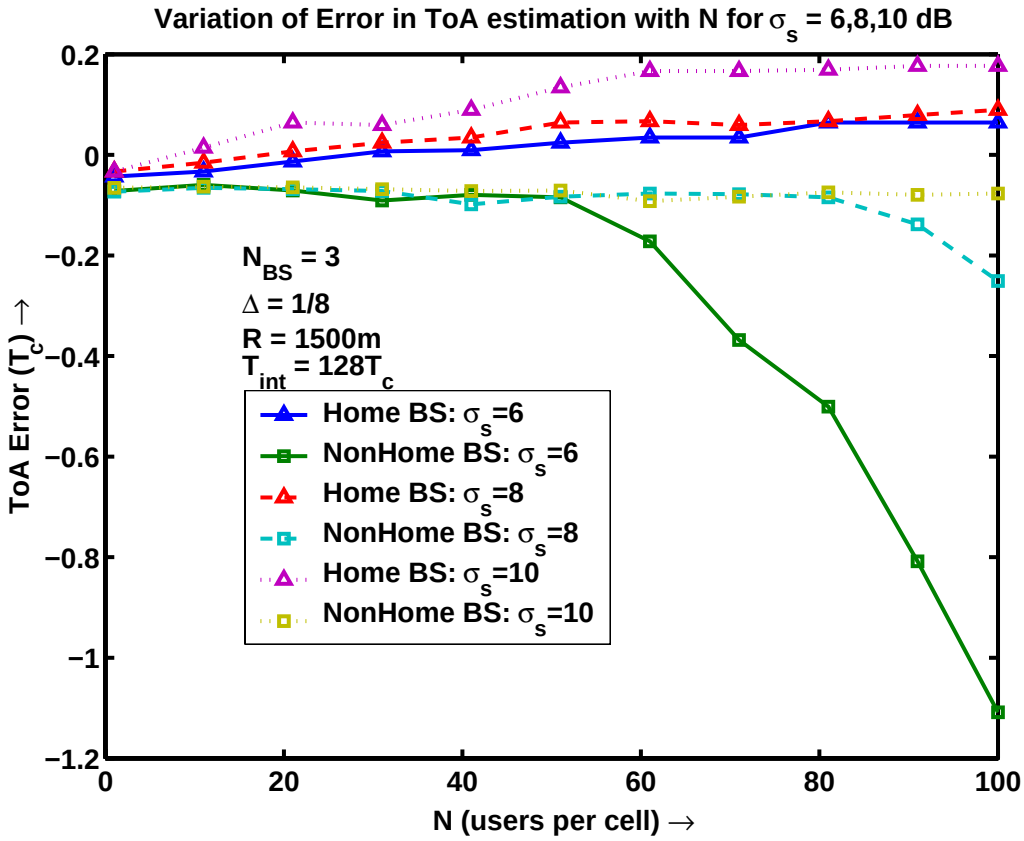

Figure 4.4: Variation of Error in ToA at Home and Non-Home BS for $\sigma_s = 6, 8, 10dB$

Table 4.2: Min and Max Error in Radiolocation for different values of σ_s

σ_s (dB)	minErr(m)	maxErr(m)	mean error(m)
6	27.399	366.33	123.35
8	26.944	124.29	72.612
10	26.955	98.915	76.633

is poorest for $\sigma_s = 10dB$, while the estimation at a non-home BS is poorest for $\sigma_s = 6dB$. The increased error in radiolocation for $\sigma_s = 6dB$ is a result of poor ToA estimation at the non-home BS's. The mean error in 2-D position estimation remains almost constant when σ_s is increased from 8dB to 10dB.

4.2 Effect of Varying the Number of Participating BS's on the Accuracy of Radiolocation

With reference to Fig. 1.14 in section 1.3.3, if only 2 BS's are used to estimate the subscriber location, due to the inaccuracies in TOA estimations, the circles would intersect at 2 different points, and an accurate estimation in such a case will be difficult. But if a third BS is introduced, as shown in Fig. 4.6 the region of uncertainty decreases and the accuracy of estimation improves. To determine the effect of the number of BS's involved in radiolocation on the accuracy of estimation, we performed an experiment where 2,3 and 4 BS's were used to estimate the subscriber location. The results are plotted in Fig. 4.5. The following conclusions can be drawn:

1. **Accuracy improves drastically if we use more than two BS's for estimation:** The accuracy of estimation improves to 72.612m from 699.32m when we employ 3 BS's to estimate the subscriber location instead of 2. Thus, it is very evident that introduction of a third estimator has a significant impact on the estimation accuracy.

2. **There is no significant improvement in the estimation accuracy when the number of BS's is increased from 3 to 4:** The mean radiolocation error improves by $\approx$ 7m when we increase the number of BS's to 4. This shows that, there is no appreciable benefit obtained when we increase the number of BS's from 3 to 4. For applications with lower accuracy requirements, 3 BS's would be sufficient for radiolocation.

Table 4.3, derived from Fig. 4.5, outlines the minimum, maximum and mean values of estimation errors for various values of N_{BS} as the number of users per cell is varied from 1 to 100, other conditions remaining same.

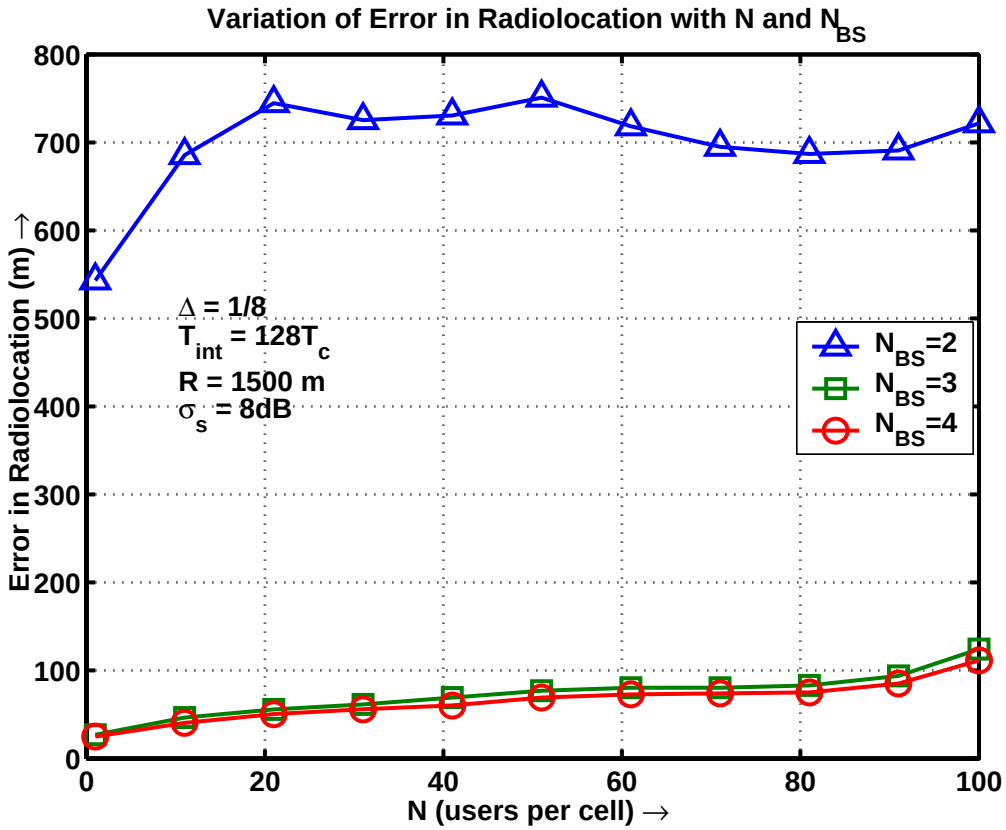

Figure 4.5: Variation of Radiolocation Error with N and N_{BS}

4.3 Effect of Varying the Early-Late Discriminator Offset on the Accuracy of Radiolocation

As earlier explained in section 1.3.3, the accuracy of radiolocation depends on the accuracy of the delay estimation technique. For our work we have used a non-coherent DLL for estimating the TOA of the received signal. The accuracy of estimating the TOA using a DLL depends on how closely the DLL can track the incoming signal, and this is defined by the parameter Δ. To study the effect of variation of Δ on the accuracy of estimation, we have performed experiments with Δ=$\frac{1}{2}$,$\frac{1}{4}$ and $\frac{1}{8}$. The results of the experiment are plotted in Fig. 4.7.
The following is concluded from the experiment:

1. **Accuracy of estimation is inversely proportional to the value of Δ:** Plot in Fig. 4.8 illustrates the performance of the DLL under varying values of Δ and N. While, the error in ToA estimation at a home BS almost remains within quarter chip period, when N increases from 1 to 100, error in ToA estimation at a non-home BS improves as DLL's with greater timing resolution capabilities are used. Hence, performance of the radiolocation system improves as DLL's with lower values of Δ are used.

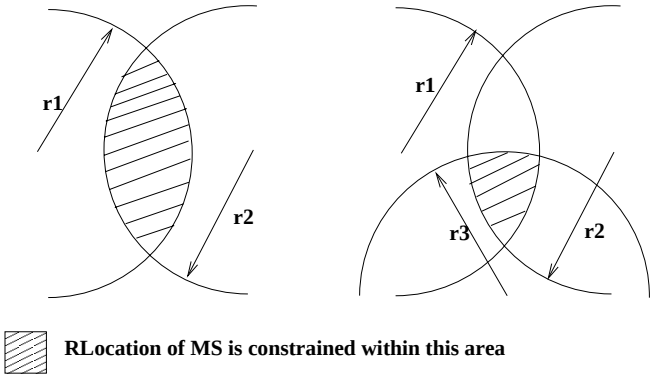

Figure 4.6: Estimating Subscriber Location Geometrically

Table 4.3: Min and Max Error in Radiolocation for different values of N_{BS}

N_{BS}	minErr(m)	maxErr(m)	meanErr(m)
2	543.1	721.64	699.32
3	26.944	124.29	72.612
4	24.695	111.4	65.393

Table 4.4, derived from Fig. 4.7, outlines minimum and maximum values of errors for different values of Δ as the number of users per cell are increased from 1 to 100, other conditions remaining same.

Table 4.4: Min and Max Error in Radiolocation for different values of Δ

Δ	minErr(m)	maxErr(m)	meanErr(m)
$\frac{1}{2}$	84.858	911.02	733.13
$\frac{1}{4}$	51.715	735.97	525.23
$\frac{1}{8}$	26.944	124.29	71.827

The mean radiolocation error reduces to 71.827m from 525.23m when, Δ is reduced from $\frac{1}{4}$ to $\frac{1}{8}$.
But, the lowest value of Δ is limited by

(a) In practice, the locally generated PN sequence will have to phase delayed to generate the early and late PN sequences. As per IS-95 standards, one chip period corresponds to 813.80 nSec. Thus, if we were to deploy a tracking loop with $\Delta=\frac{1}{16}$, the requirement

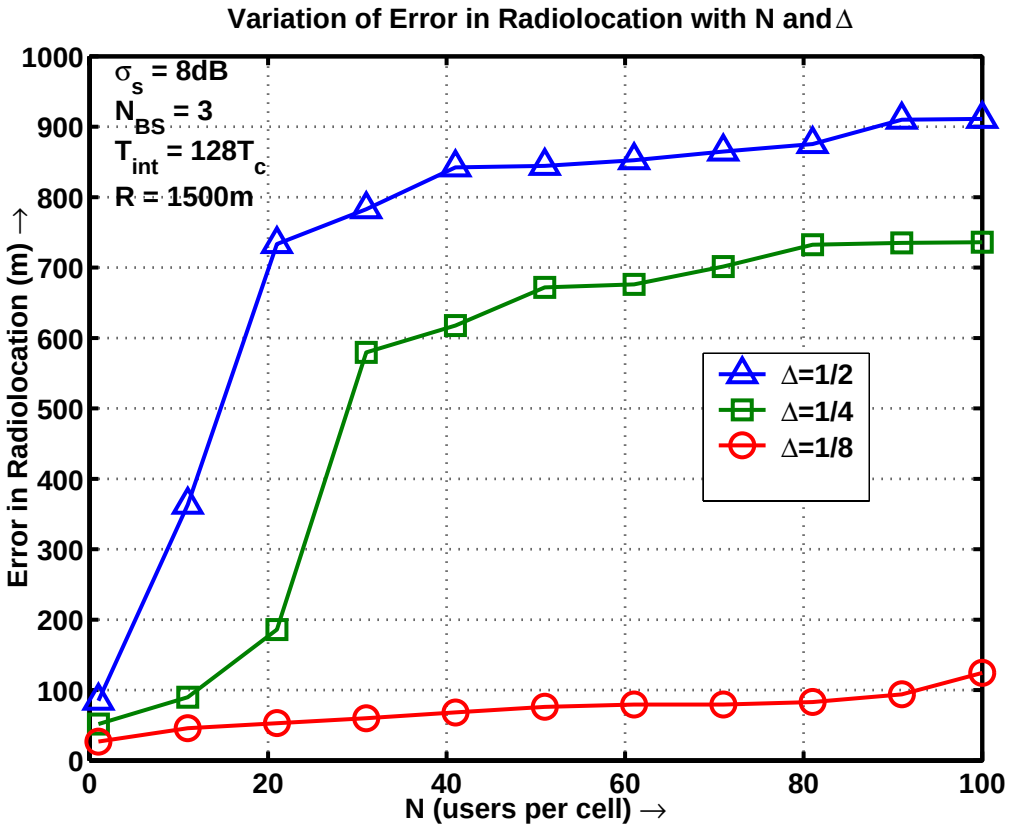

Figure 4.7: Variation of Radiolocation Error with N and Δ

on the timing resolution capability of the hardware will be

$$\begin{aligned} \Delta t &= T_c \times \Delta \\ &= \frac{813.02}{16} nSec \\ &= 50.8626 nSec \end{aligned}$$

Implementing such high precision tracking loops is both challenging and expensive.

(b) If the DLL employ's a serial search technique, it will have to search through all potential code delays until the correct delay is identified. Suppose, the incoming PN sequence is delayed by T_c. If $\Delta = 1/k$, there are k potential delay values between 0 and T_c that the DLL will have to search through before it can lock to the subscriber signal. Thus, the size of the set of potential delays increases as the the value of Δ decreases. The bigger the set of potential delays, the longer will it take for the tracking loop to achieve a lock. The situation becomes more complicated, if we are also estimating the velocity of the subscriber. The set of potential delays, soon transforms into a 2D matrix defining the set of potential delays and velocities. A serial search technique would be inefficient for such cases. More smarter search techniques need

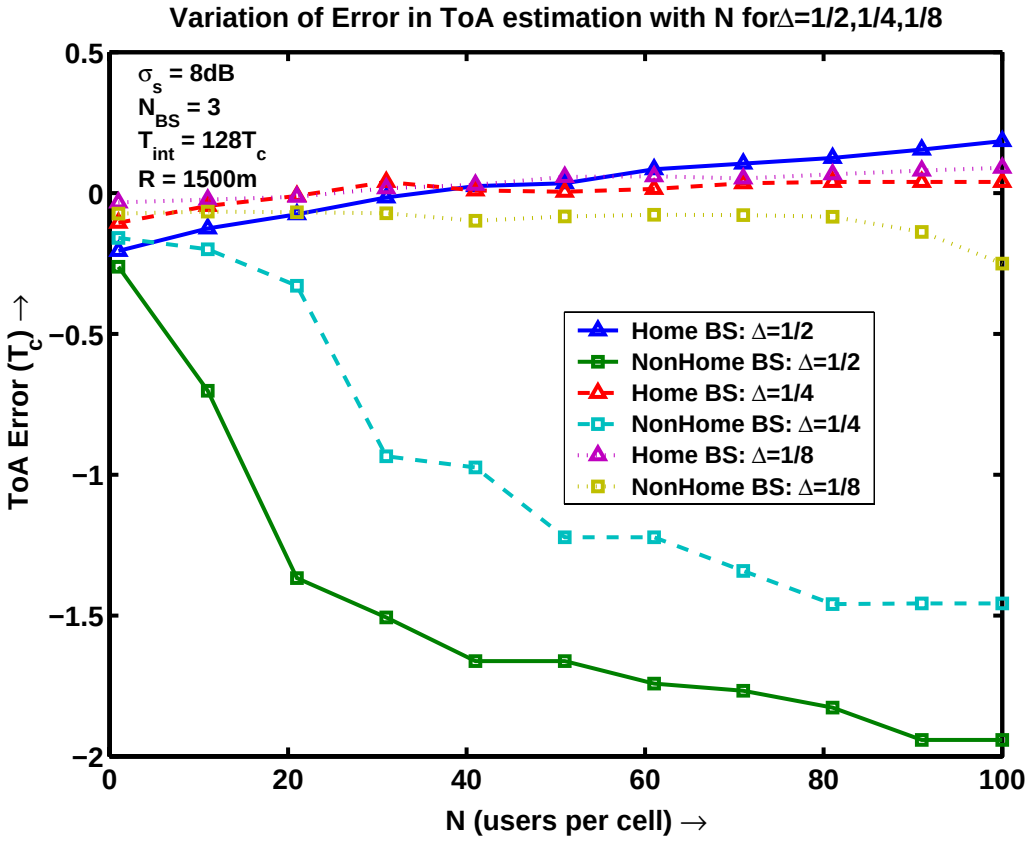

Figure 4.8: Variation of Error in ToA at Home and Non-Home BS for $\Delta = 1/2, 1/4, 1/8$

to be employed.
Thus, the time taken for estimation also puts a lower limit on the value of Δ.

2. **Accuracy falls as number of users per cell increases :** As can be seen from Fig. 4.7, the accuracy of estimation, falls as the number of users per cell increases. This is because of the degradation of SNR with increasing number of users per cell, as can be seen in Fig. 4.1 and Fig. 4.2.

4.4 Effect of Varying the Cell Size on the Accuracy of Radiolocation

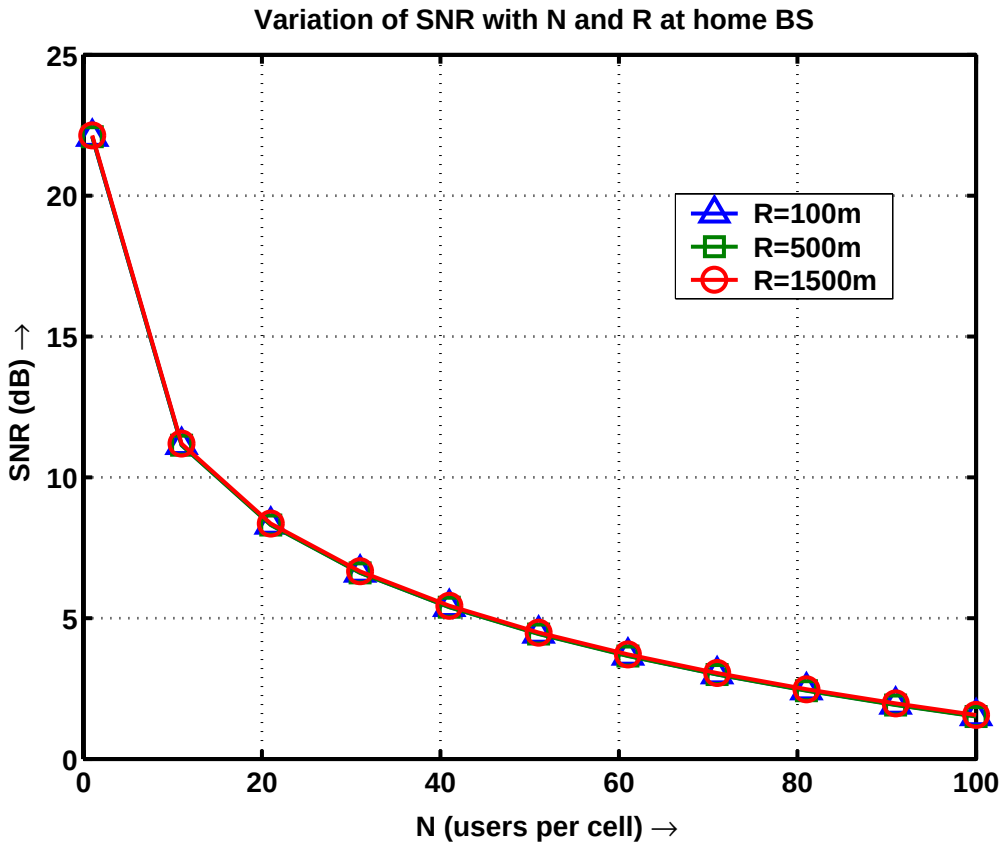

Figure 4.9: Variation of SNR at Home BS with N and R

All the earlier experiments were carried out with cells of radius 1500m. To study the effect of cell size on the accuracy of estimation, we simulated coverage area's with cell sizes 100m and 500m. Simulations were carried out under the following situation:

- $\Delta = \frac{1}{8}$

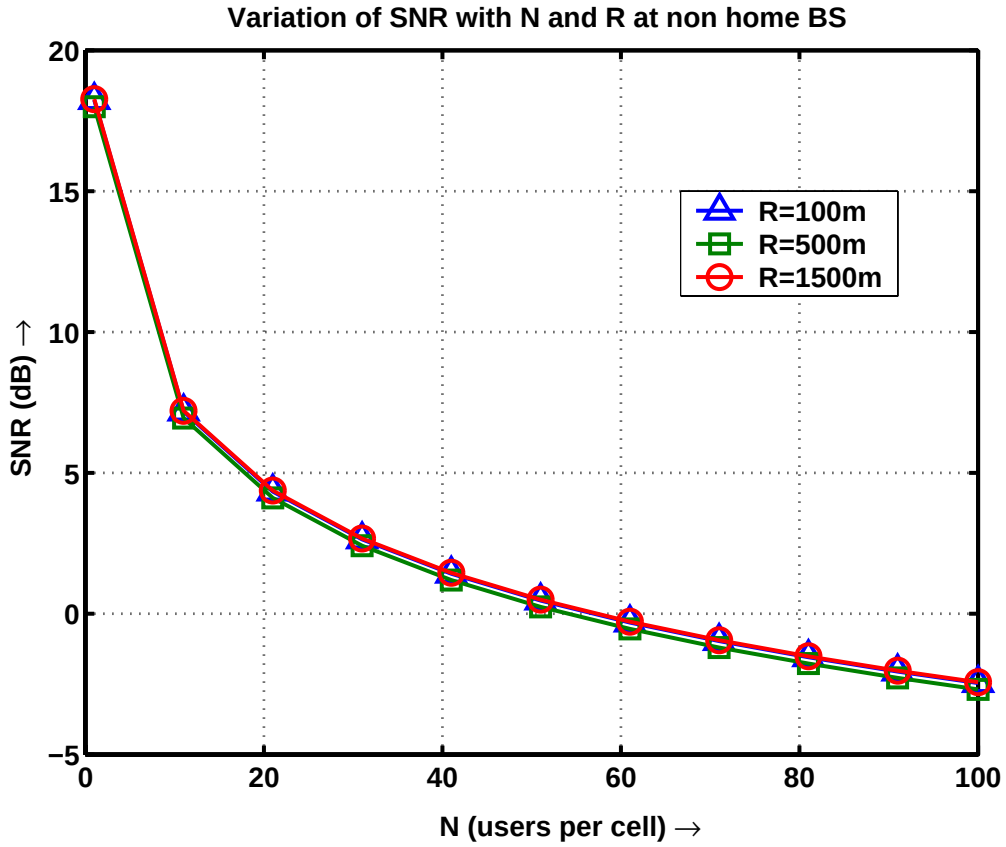

Figure 4.10: Variation of SNR at Non-Home BS with N and R

- $\sigma_s = 8dB$
- Number of BS's involved in radiolocation = 3
- Number of users varied from 1 to 100 in steps of 10.

The results were then compared with the results of the experiment carried out under identical situation but using cells of radius 1500m. The results indicate that:

1. **Under perfect power, the degradation in SNR with number of users is independent of the cell size:** A plot of SNR-vs-number of users per cell is shown in Fig. 4.9 and Fig. 4.10. As can be seen from the plots, the values of SNR at the home and non-home BS, do not vary much with the cell size.
   For a home BS, Equ. (3.11) gives the total amount of interference at a home BS. The equation is independent of the radius of a cell. Similarly, for a non-home BS Equ. (3.12) gives the total amount of interference at a non-home BS. Even this equation is independent of the radius of a cell. The signal strength and the amount of interference both depend on the value of κ_{ij}, given by Equ. (2.24). As users are assumed to be power controlled, each

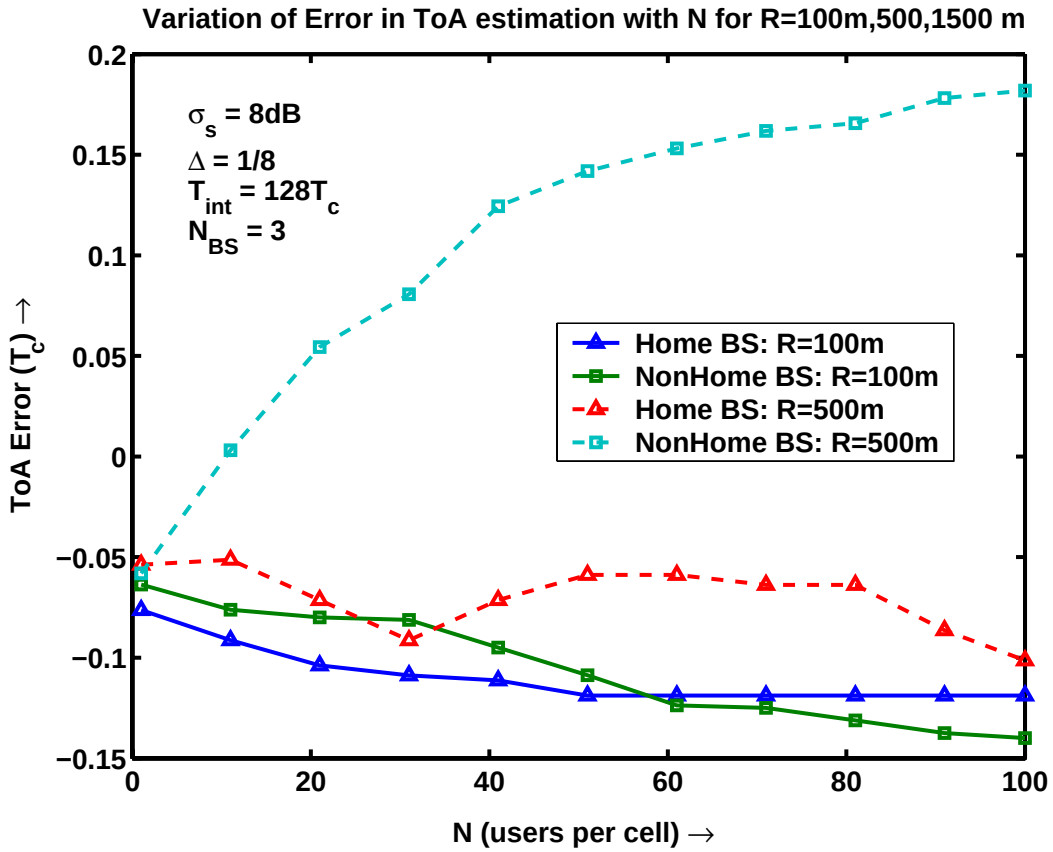

Figure 4.11: Variation of Radiolocation Error with the R and N

user transmits a signal level proportional to its distance from the home BS. Hence, SNR being a ratio of signal energy to interfering power, is independent of the cell radius.

2. **Under perfect power control, accuracy of estimation is better with smaller cells:** Estimation of ToA would be accurate if it lies within the tracking range of the DLL. For bigger cells, the delay experienced by a signal in reaching the non-home BS is large. Plot in Fig. 4.12 gives a comparison of the error's in ToA estimation at a home and non-home BS for cells of radius 100m and 500m. The error in estimation at a non-home BS is better for cells of radius 100m than for cells of radius 500m. But, at the same time, the ToA estimation at a home BS is better for cells with radius 500m. This is a result of the minimum value of delay that a DLL can estimate. For cells with smaller radius, the delay experienced by the signal while traveling to a home BS becomes comparable to the timing resolution of the DLL, and hence the probability of an incorrect estimation increases.
   For the experiment conducted with cells of radius 100m, 500m and 1500m it is found that accuracy of radiolocation is best for cells of radius 100m. Table 4.5 lists the observed values of minimum, maximum and mean values of error.

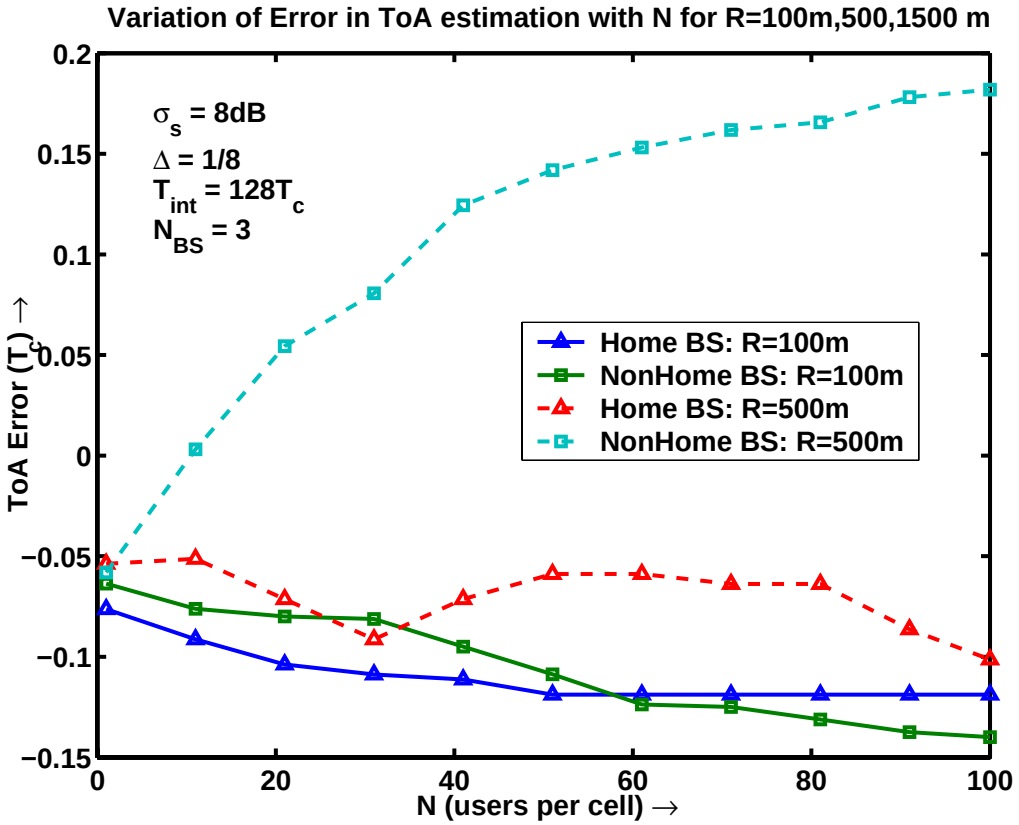

Figure 4.12: Variation in ToA Estimation with the R and N

Table 4.5: Min and Max Error in Radiolocation for different values of R

R	minErr(m)	maxErr(m)	meanErr(m)
100	21.766	32.325	31.9
500	24.062	83.485	61.259
1500	26.944	124.29	72.612

Chapter 5

Conclusion

Through our work, we have investigated the possibility of accurate subscriber location in CDMA cellular networks in the presence of multiple access interference. Earlier works have ignored the effect of non-orthogonality of the PN codes on the estimation accuracy. They usually consider the case of a single MS with no interferer's, which is not a practical assumption. But, in our work, we have studied the effect of number of interferer's on the accuracy of estimation by varying the number of users in every cell from 1 to 100. To study the effects of multiple access interference on the accuracy of estimation, we have assumed the presence of a LoS component between the MS and the BS. We have studied the effect of MAI in conjunction with:

1. Varying shadowing environments
2. Varying tracking capability of the DLL
3. Varying number of BS's participating in radiolocation
4. Varying cell sizes

For a given value of σ_s, the estimation improves by using a smaller early-late discriminator offset Δ. Also, for a set value of Δ, the error in estimation increases with the number of users. As can be seen from the results outlined in table 4.4, estimating subscriber locations with systems of lower values of Δ is advantageous as the maximum and mean error in estimation dip as Δ decreases. But, the lowest value of Δ is bounded by the hardware complexity of the tracking loop and time required for estimation.
For 2-D location, the location error is reduced by increasing the number of BS's used in the location process. Also, under perfect power control, cell sizes effect the accuracy of estimation. Table 4.5 shows that the maximun and mean error decrease as the cell size decreases. But, the minimum and maximum cell size a detection system can support is limited by

- The early-late discriminator offset
- The minimum and maximum trackable delay by the employed ToA estimator

respectively. For example consider an IS-95 CDMA network with T_c=813.02nSec. If $\Delta = \frac{1}{4}$, the minimum cell size is computed as

$$\begin{aligned} R_{min} &= T_c \times \Delta \times c \\ &= 60.9765m \end{aligned}$$

These results are not vis-a-vis applicable to a microcellular environment.

The results obtained through the simulations carried out under different conditions are encouraging and show that radiolocation is possible in a CDMA system, even when multiple access interference is present.

Chapter 6

Applications

Emergency services and safety concerns have driven the development of location-based services. Over one-third of emergency calls in the United States are made from mobile phones. United States and the European Union, laws require wireless service providers to implement emergency location services. These services communicate the precise geographic location of a wireless device to the proper authorities when it is used to make an emergency call.
With the resources for location-based emergency services in place and growing interest in target detection for military applications, additional applications become possible. The rapidly growing demand for consumer-oriented location based services creates new opportunities for wireless service providers. HP and Openwave recently conducted a research finding survey identifying the consumer interest in radiolocation services [29]. The survey identified the various applications for the radiolocation.

6.1 Location-based Services

6.1.1 Get Directions

With positioning capability, this service would provide precise directions from the mobile users current location. Text instructions accompanied by a customized map guide mobile users to their destination. Content quality is crucial to a successful implementation. Directions should account for mode of transportation (e.g., pedestrian, public transit, private vehicles) and address safety concernsvoice input and verbal instructions facilitate use by drivers.

6.1.2 Find Nearest

This service combines aspects of the get directions feature with the functionality of the yellow pages. Subscribers can identify a resource of particular interest close to their current location and obtain directions and other relevant information about it. Mobile users can find the closest movie theater, check its schedule, and purchase tickets; or they can search for a particular type of restaurant, review its menu, and make reservations. Hotels, hospitals, ATMs, gas stations, parking, and moreall there for the asking. Again, content quality is crucialinformation must be accurate and thorough.

6.1.3 Concierge

Of particular interest to frequent travelers and mobile professionals, this service automatically provides a variety of local information when the subscriber arrives in a new citylocal weather, travel tips, restaurants, games, events, and other items of interest. Some users would subscribe to this service regularly, others might prefer to adopt it only for short periods while traveling.

6.1.4 Alerts

This service automatically provides the subscriber with information updates on topics requested by the user. There is specific interest in commuter information, especially updates about traffic conditions. Entertainment also drew significant interestannouncements of concerts, shows, and other special events, ticket sales and special deals. Other alert categories include school closings, flight delays, weather, and sports news. Alert services show the most promise in cities with traffic problems and extensive entertainment options.

6.1.5 Friend Finder

This service provides position information for other mobile users, allowing subscribers to locate their friends or share their own location. Position information can be plotted on a map or displayed as an address. Privacy and security issues are paramount for this type of serviceindividual subscribers must be able to define their own preferences regarding who is authorized to know their position, and when.

6.1.6 Child Finder

Similar to friend finder, this service allows parents to keep track of their younger children. It periodically compares the location of a small child (or specifically, a mobile device carried by the child) against a schedule and geographic area set by the parent. The service alerts the parent if the mobile device is not where expected. In this manner, parents are reassured that their small children are safe and where theyre supposed to be. Because of sensitive trust and privacy issues, however, it may not be appropriate for teens.

6.1.7 Bundled Safety Package

Research showed considerable interest in bundled safety services. Location information enhances roadside assistance and emergency calls; and traffic alert and child finder services add value to basic safety functionality.

6.1.8 Additional Services

Opportunities exist for further expanding and enhancing these location-based services. Interactive games have a measure of appeal for young adults and teens. Other possibilities include a

service for tracing lost or stolen phones, book-marking locations as landmarks for directions, even location-based dating services.

Chapter 7

Future Work

Wireless communications constitute one of the most vital and dynamic areas of the technology market. With over 500 million cellular phones sold around the world, the last year, and ever increasing consumer database, emphasis on research in the field of radiolocation is ever increasing. A lot of work has already been done in this field, but to enable a gamut of location based services aimed at providing security, safety and consumer satisfaction, this area is an active field of research.
A few of the active research areas are:

Indoor Radiolocation The problem of indoor radiolocation is severe than the outdoor radiolocation, because the signal in an indoor environment undergoes multiple reflections. This leads to a severe multipath and radiolocation in such an environment is a challenging task. Research groups are investigating the use of wideband position location systems, like UWB for indoor radiolocation.

Dynamic user location Most of the current work in radiolocation investigate application of radiolocation techniques for static subscribers. But, this restriction on user mobility is unrealistic. In reality, the user may be traveling at different speeds. This degrades the link quality between the MS and BS. In addition to fading, multipath, and NLOS propagation, the received signal will have Doppler shifts. Accurate estimation of TOA under such condition is challenging.

Mobility Management It is very necessary to develop a model of the user mobility behavior in wireless networks. The developed model can be used to estimate the rate at which the location of the subscriber must be updated. An accurate modeling is essential, as the rate of updation would determine the network traffic and the necessary processing power required at the BS's.

Development of receiver's Radiolocation using TOA involve non-home BS's. The SNR at a non-home BS is very low as compared to the SNR at home BS. Estimation of TOA under low SNR, multipath, fading and NLOS propagation is difficult. Hence, some attention is required to enhance the detection and processing capabilities of receivers.

Bibliography

[1] J. Caffery, Jr., and G. Stuber, "Subscriber Location in CDMA Cellular Networks," *IEEE Trans. Vehic. Tech.,* vol. VT-47 No-2, May 1998, pp. 406-15

[2] W. Figel, N. Shepherd, and W. Trammell, "Vehicel Location by a Signal Attenuation method," *IEEE Trans. Vehic. Tech.,* vol. VT-18, Nov. 1969, pp.105-110

[3] M. Hata and T. Nagatsu, "Mobile Location Using Signal Strength Measurements in a Cellular System," *IEEE Trans. Vehic. Tech.,* vol. VT-29, May 1980, pp. 245-51

[4] W. Smith, Jr., "Passive Location of Mobile Cellular Terminals," *Proc. IEEE Int'l. Carnahan Conf. Security Tech.,*" 1991, pp. 221-25

[5] W. C Jakes, "*Microwave Mobile Communication*," IEEE Press, 1994

[6] J. Parsons, "*The Mobile Radio Propogation Channel*," Halsted Press, 1992

[7] M. Gans, "A Power Spectral Theory of Propogation in the Mobile Radio Environment," *IEEE Trans. Vehic. Tech.,* vol. VT-21, Feb 1972, pp. 27-38

[8] Joseph C. Liberti, Jr., Theodore S. Rappaport, "Smart Antennas for Wireless Communications: IS 95 and Third Generation CDMA Applications," *Prentice Hall communications engineering and emerging technologies series.,* 1999

[9] H. Saarnisaari, "TLS-ESPIRIT in a Time-Delay Estimation," *Proc. IEEE VTC*, 1997, pp. 1619-23

[10] R. Ilts, "Joint Estimation of PN Code Delay and Multipath Using Extended Kalman Filter," *IEEE Trans. Commun.,* vol. 38, Oct. 1990, pp. 1677-85

[11] H. So and P. Cheng, "Target Localisation in Presence of Multipaths," *Elect. Lett.,* Feb. 4 1993, pp. 293-94

[12] K. Krizman, T. Biedka, and T. Rappaport, "Wireless Position Location: Fundamentals, Implementation Strategies, and Sources of Error", *Proc. IEEE VTC*, 1997, pp. 919-23

[13] L. Dumont, M. Fattouche, and G. Morrison, "Super-Resolution of Multipath Channels in a Spread Spectrum Location System," *Elect. Lett.,* Sept. 15 1994, pp. 1583-84

[14] M. Silventoinen and T. Rantalainen, “Mobile Station Emergency Locating in GSM,” *Proc. IEEE Int’l Conf. Pers. Wireless Commun.,* 1996, pp. 232-38

[15] M. Wyile and J. Holtzman, “The Non Line of Sight Problem in Mobile Location Estimation,” *Proc. IEEE ICUPC,* 1996, pp. 827-31

[16] Theodore S. Rappaport, “Wireless Communications: Principles and Practice,” Prentice Hall PTR, 1996

[17] K. S. Gillhousen, I. M. Jacobs, R. Padovani, A. J. Viterbi, L. A. Weaver, and C. E. Wheately, “On the capacity of a cellular CDMA system,” *IEEE Transactions on Vehicular Technology,* vol. 40, No. 2, pp. 303-312, May 1991

[18] Robert G. Akl, Manju V. Hegde, Mort Naraghi-Pour, Paul S. Min, “Multi-Cell CDMA Network Design,” *IEEE Transactions on Vehicular Technology,* vol. 50, No. 3, pp. 711-722, MAY 2001

[19] R. G. Akl, M. V. Hegde, A. Chandra, and P. S. Min, “CCAP: CDMA Capacity Allocation and Planning,” Tech. Rep., Washington University, April 1998

[20] Morrow, R. K., Jr., and Lehnert, J. S., “Bit-to-Bit Error Dependence in Slotted DS/SSMA Packet Systems with Random Signature Sequences,” *IEEE Transactions on Communications,* vol. 37, No. 10, Oct 1989

[21] Gordon L. Stuber “Principles of Mobile Communication,” 2^{nd} edition, Kluwer Academic Publishers

[22] Roger L. Peterson, Rodger E Ziemer, David E Borth, “Introduction to Spread Spectrum Communications,” *Prentice Hall Publications*

[23] Willian C. Y. Lee, “Mobile Cellular Telecommunications, Analog and Digital Systems, 2nd Ed,”’ *McGraw-Hill, Inc*

[24] http://www.mathworks.com/access/helpdesk/help/techdoc/matlab.html

[25] http://www.mathworks.com/access/helpdesk/help/toolbox/simulink/

[26] http://www.igi.tugraz.at/lehre/MLA/WS01/asamin.html

[27] http://www.ingber.com/ASA-README.html

[28] http://www.library.cornell.edu/nr/bookcpdf/c10-9.pdf, pp.444-455

[29] http://h71028.www7.hp.com/enterprise/downloads/ESGwireless.34.pdf

Vita

Rohit Sharma was born in the city of Kalyan, a suburb of Mumbai, in the state of Maharashtra, India. He graduated from High School in April 1997. In the Fall of 1997, he enrolled in the department of Electronics and Telecommunications at the Mahatma Gandhi Mission's college of Engineering and Technology, Mumbai University, Navi Mumbai, and graduated with a first class in fall 2001 with a Bachelor of Engineering degree. He then worked for two years as a design and development engineer at Aplab Limited, a leading design house at Thane, Mumbai. Later in the fall of 2003 he enrolled in the Department of Electrical and Computer Engineering at Louisiana State University to puruse graduate studies and is expected to get his Master of Science in Electrical Engineering degree in Spring 2005.